Geological Materials Research
Volume 3
Number 1
December 17, 2001

Metapelite phase equilibria modeling in MnNCKFMASH: The effect of variable Al_2O_3 and MgO/(MgO+FeO) on mineral stability

Douglas K. Tinkham, Carlos A. Zuluaga, Harold H. Stowell

Department of Geological Sciences, University of Alabama, Tuscaloosa, AL 35487-0338, USA
<tinkh001@bama.ua.edu>

Abstract

A series of MnO-Na_2O-CaO-K_2O-FeO-MgO-Al_2O_3-SiO_2-H_2O (MnNCKFMASH) metapelite pseudosections highlights the dependence of predicted mineral assemblages on bulk rock Al_2O_3 and Mg# (MgO/(MgO+FeO)). T-X_{Al} pseudosections portray the dependence of staurolite, biotite, and aluminum silicate on Al_2O_3 content, allowing the distinction between high-Al and low-Al pelite, as commonly portrayed with KFMASH modeling. The MnNCKFMASH system also shows the effect of Al_2O_3 on plagioclase and zoisite stability, which cannot be done in the KFMASH system. Comparison of MnNCKFMASH to KFMASH pseudosections highlights the consequence of ignoring the important rock constituents MnO, Na_2O, and CaO when constructing pseudosections. KFMASH cannot model important phases such as plagioclase and zoisite, and there are significant differences in predicted garnet, biotite, and chloritoid stability in the two different systems. In particular, KFMASH does not model garnet stability appropriately at low pressures and temperatures because it cannot account for the stabilizing effect of Mn. The comparisons also show that the method of calculating a KFMASH bulk rock composition equivalent to a real rock composition is problematic and has significant implications for the predicted pseudosection assemblage stability.

Comparison of the MnNCKFMASH pseudosections to natural assemblages observed in the Waterville Fm., Maine, indicates that the MnNCKFMASH system comes very close to modeling naturally developed mineral assemblages successfully. The only major discrepancy between predicted and observed assemblages is the inability to predict the paragenesis staurolite + andalusite using an average or natural Waterville Fm. composition.

Garnet thermobarometric results from the Waterville Fm. are in poor agreement with pseudosection topology for an average Waterville Fm. composition. This suggests that if quantitative P-T path information is to be derived through a combination of pseudosections and thermobarometry, samples will have to be investigated on an individual basis in more detail than was done in this study.

Keywords: metapelite, phase equilibria, pseudosections, mineral assemblage, thermodynamics, bulk composition, Waterville Fm., metamorphic petrology, thermobarometry

Introduction

The development of large thermodynamic data sets including properties for common metapelite minerals allows calculation of stability limits for minerals and mineral assemblages in P-T space. These calculations are typically performed in relatively simple chemical systems with a limited number of phases considered. Natural rocks inevitably contain phases and/or phase components outside the chemical system chosen for modeling. Thus, it is critical to test the applicability of model systems to real rocks by quantitative comparisons with natural mineral assemblages and pressure-temperature conditions. A major concern involved in modeling is the effect of bulk rock composition on the P-T stability of minerals and hence assemblages. Therefore, the chemical system appropriate for quantitative modeling of any particular rock is dictated by mineralogy and bulk rock composition. Ignoring elements that affect mineral stability degrades the applicability of quantitative phase equilibria modeling to real rocks.

Previously, the lack of end-member thermodynamic data, and perhaps more importantly, the lack of activity models to describe mixing in solid solution phases limited the ability of models to predict mineral stability for natural rocks. Although activity models remain a significant problem, internally consistent thermodynamic data are now available for many phases (Berman, 1988; Holland and Powell, 1985, 1990, 1998; Gottschalk, 1997; Spear et al., 2001; Pattison et al., in press). Existing thermodynamic data therefore allow modeling of rocks in chemical systems approaching the complexity of natural rock compositions.

The stability of invariant, univariant, and divariant mineral assemblages in P-T space is typically investigated with petrogenetic grids (projection of univariant lines and invariant points in P-T-composition space onto the P-T plane). The KFMASH system is commonly used to model pelitic rocks with petrogenetic grids (e.g., Thompson, 1976; Pattison and Tracy, 1991; Spear, 1993), and to first order provides a basis for understanding the sequence of mineral assemblages developed in pelitic rocks with varying P-T conditions.

The importance of petrogenetic grids, and the ability to use simplified petrogenetic grids while making observations in the field to place constraints on the P-T conditions of metamorphism is discussed by Pattison and Tracy (1991). However, examination of AFM diagrams clearly indicates that the actual assemblage expected for a particular rock is highly dependent on the effective bulk composition available to the reacting assemblage of minerals and fluid. At any point on a petrogenetic grid, the most stable assemblage for a particular composition may indeed be a tri-, quad-, or higher variance assemblage. The information needed to determine which assemblage will be stable for a particular composition is not displayed on a petrogenetic grid, and therefore, the application of grids to individual samples to discern expected assemblages at varying P-T conditions is not straightforward, especially in chemically complex systems (e.g., Worley and Powell, 1998). The use of pseudosections (Hensen, 1971; Powell et al., 1998) alleviates this problem by portraying only the assemblage that is theoretically most stable, whatever its variance, at any given P-T condition for a specified bulk composition.

Although KFMASH is commonly used for pseudosection modeling, the use of more complex chemical systems is increasing. Mahar et al. (1997) used MnKFMASH and Symmes and Ferry (1992) used MnNKFMASH to display the effect of Mn on metapelite phase stability. Worley and Powell (1998) used NCKFMASH to portray singular equilibria for common pelite mineralogy. White et al. (2000) added TiO_2 and Fe_2O_3 to KFMASH (KFMASHTO) to consider Fe-Ti oxide equilibria. Stowell et al. (2001), Vance and Holland (1993), Vance and Mahar (1998), and Tinkham and Stowell (2000) used the MnNCKFMASH system to derive garnet growth P-T paths from amphibolite facies metapelites. This study uses pseudosections to address the role of variable bulk rock Al_2O_3 and MgO/(MgO+FeO) content on metapelite assemblage stability in the model system MnNCKFMASH. Although this system does not allow modeling of potentially important phases such as carbonates, sulfides, Fe-Ti oxides, graphite, a COH fluid, or Ti and Fe3+ end-member phases, the major rock forming minerals in typical pelites can be modeled. The advantages of this system over simpler systems (e.g., KFMASH, MnKFMASH, and NCKFMASH) for pseudosection modeling includes its ability to model quantitatively both garnet and Na and Ca bearing phases commonly found in metapelites (e.g., plagioclase and zoisite/clinozoisite). The KFMASH system is appropriate for modeling Fe-Mg partitioning relationships and isograds based on Fe-Mg phases, but cannot quantitatively model garnet composition or the effect of Al-rich Na and Ca bearing phases on aluminum silicate stability. Many metapelites contain garnet and Na and Ca bearing phases; therefore, for many purposes MnNCKFMASH is the minimum system required to apply quantitatively pseudosections to natural metapelites. We present MnNCKFMASH pseudosections calculated for an average biotite zone metapelite composition, Waterville Fm., Maine, and discuss the applicability of such an average pseudosection to the

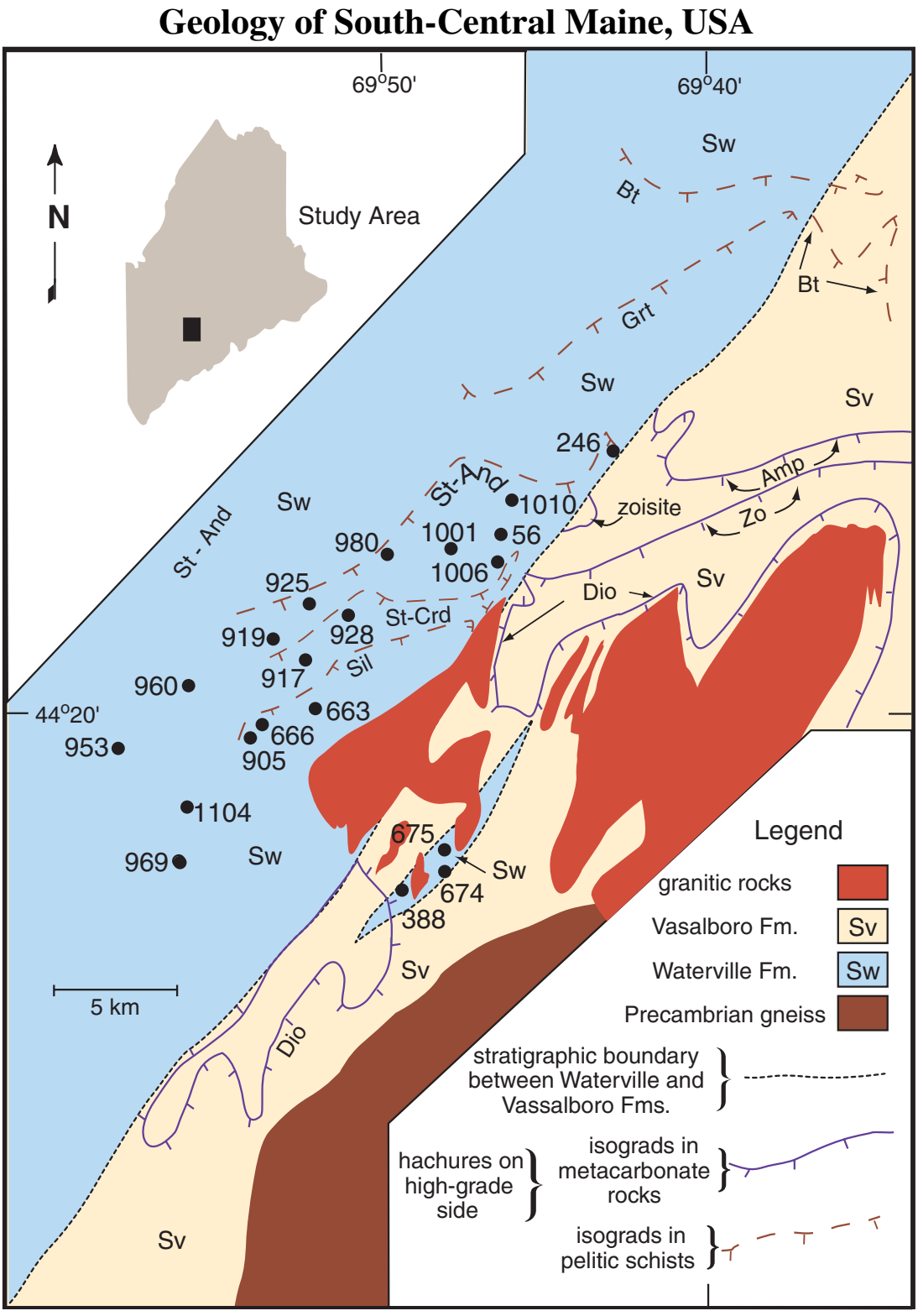

Figure 1. Geologic map showing the Waterville Fm., Maine, metamorphic isograds, and sample locations for thermobarometry. Modified from Ferry (1980, 1982).

natural suite of assemblages developed in the biotite through sillimanite zones of metamorphism. In addition, garnet thermobarometric results for a select group of Waterville Fm. samples are compared to the average biotite zone pseudosection to assess consistency between pseudosections and conventional thermobarometry. We conclude that the MnNCKFMASH system is appropriate for modeling mineral stability for typical metapelite compositions.

Methodology

An average of eight bulk rock compositions from the biotite zone (reported in Ferry, 1982) for the Waterville Fm., Maine (Fig. 1), was used to calculate P-T pseudosections from 425-700 °C and 1-10 kbars. This average Waterville biotite zone composition (AWBZ) plots in the low-Al pelite stability field of Spear (1993) in an AFM projection when the composition is projected from albite. The AWBZ is compared to the Mahar et al. (1997) average pelite, Symmes & Ferry (1992) average pelite, and an average Dalradian pelite composition (Atherton & Brotherton, 1982) in Table 1 and Figure 2. In this study, quartz and H_2O are considered to be in excess, so for comparison to pelite compositions of previous studies, all analyses were recalculated on a hydrous-free and $FeO_{(total)}$ basis in the nine component system MnNCKFMASH. Compared to the other pelite compositions, the AWBZ has higher FeO, MgO, MnO, and MgO/(MgO+FeO), but lower Al_2O_3 and slightly lower Na_2O and K_2O. The CaO content is comparable to that of the Mahar et al. (1997) composition, higher than the Dalradian composition (Atherton and Brotherton, 1982), and significantly lower than the Symmes and Ferry (1991) composition.

KFMASH and MnNCKFMASH pseudosections for the AWBZ are compared to show the effect of MnO, Na_2O, and CaO on predicted metapelite mineral stability and address the problem of deriving a KFMASH composition equivalent to that of a natural sample. A pseudosection corresponding to the AWBZ with increased Al content was constructed to illustrate the effect of variable Al on the P-T stability of MnNCKFMASH assemblages. This increased Al composition (High-Al AWBZ, Table 1) was derived from the AWBZ by increasing Al_2O_3 from 37.99 to 45.80 mole %, and decreasing all other components proportionally. The Al_2O_3 content of the Symmes and Ferry, Mahar et al., and Dalradian compositions fall between the AWBZ and High-Al AWBZ. The Al_2O_3 of the High-Al AWBZ was chosen to be slightly greater than that of the Dalradian pelite (Table 1) and to be greater than the low-Al/high-Al pelite boundary (discussed below). In addition, a P-T pseudosection for sample 980A (Table 1) from the staurolite-andalusite zone is presented. T-X (temperature-composition) pseudosections calculated at a constant pressure appropriate for the Waterville samples are presented to illustrate the progressive change in assemblages as a function of changing bulk composition. The T-X_{Al} pseudosections highlight the progressive change in assemblage stability with increased Al content from that of the AWBZ at 3.5 and 5.0 kbars. T-$X_{Mg\#}$ (MgO/(MgO+FeO)) pseudosections illustrate the effect of changing Mg and Fe content relative to the AWBZ and High-Al AWBZ at 3.5 kbars. The AWBZ and 980A pseudosections are compared to the suite of mineral assemblages observed near Waterville, Maine, in the biotite, garnet, staurolite-andalusite, staurolite-cordierite, and sillimanite zones. Finally, garnet-biotite (GaBi) and garnet-aluminum silicate-plagioclase-quartz (GASP) thermobarometric results are used to assess the correspondence between calculated garnet-rim P-T conditions, assemblages observed in the Waterville Fm., and predicted mineral assemblages from the MnNCKFMASH pseudosections.

Pseudosections presented in this paper show the distribution of mineral assemblages in either P-T or T-X space, and the boundaries between assemblage fields represent the location where the mode of a single phase goes to zero. An exception to this rule occurs when univariant reaction lines are stable, along which the mode of two phases simultaneously go to zero. At the point where two assemblage field boundaries intersect, the mode of two phases goes to zero. Since the boundaries of assemblage fields really represent a particular modal contour line (mode zero line), we occasionally refer to these boundaries as isopleths (e.g., Grt-in isopleth, zero mode isopleth), implying that the boundary represents the location where the mode of a phase goes to zero. All pseudosections were calculated using the program THERMOCALC (v. 2.7; Powell and Holland, 1988; Powell et al., 1998) and the 1998 thermodynamic data set of Holland and Powell (1998; th pdata file created Sept. 26, 1997). Quartz and an H_2O fluid phase are considered as in excess, and are present in all assemblages discussed below. Mineral abbreviations follow those of Kretz (1983). Thermobarometry calculations utilize the same thermodynamic data set and activity models as the pseudosections. Phases considered in this study and activity models are presented in Appendix 1. Thermobarometry methods are presented in Appendix 2.

KFMASH and MnNCKFMASH AWBZ Pseudosections

Derivation of KFMASH compositions

Previous metapelite modeling clearly indicates that addition of Mn to the KFMASH system substantially increases predicted garnet P-T stability (e.g., Trzcienski,

Table 1. Bulk rock compositions.

Pelite	Waterville AWBZ	Waterville High-Al	Waterville 980 A	Symmes & Ferry[1]	Mahar et al.[2]	Dalradian[3]
			Wt. % Oxides			
SiO_2	60.78	60.14	52.43	59.77	59.80	64.20
Al_2O_3	16.88	23.04	20.78	16.57	16.57	16.69
FeO (total)	6.87	6.79	8.42	5.88	5.81	4.45
MgO	3.44	3.41	3.60	2.62	2.62	2.13
MnO	0.13	0.13	0.16	0.07	0.10	0.10
CaO	1.21	1.20	2.70	2.17	1.09	0.84
Na_2O	1.65	1.63	2.59	1.73	1.73	2.11
K_2O	3.70	3.66	4.68	3.53	3.53	3.38
Total	94.66	100.00	95.36	92.34	91.25	93.90
			Molecular Proportions			
SiO_2	69.89	66.98	61.24	70.59	71.61	74.55
Al_2O_3	11.44	15.12	14.30	11.53	11.69	11.42
FeO (total)	6.60	6.33	8.23	5.81	5.82	4.32
MgO	5.90	5.65	6.27	4.61	4.68	3.69
MnO	0.13	0.12	0.16	0.07	0.10	0.10
CaO	1.49	1.43	3.38	2.75	1.40	1.05
Na_2O	1.84	1.76	2.93	1.98	2.01	2.38
K_2O	2.71	2.60	3.49	2.66	2.70	2.50
Total	100.00	100.00	100.00	100.00	100.00	100.00
			Molecular Proportions (SiO_2 free)			
Al_2O_3	37.99	45.80	36.91	39.21	41.18	44.87
FeO (total)	21.93	19.16	21.23	19.75	20.49	16.98
MgO	19.59	17.13	16.17	15.69	16.47	14.49
MnO	0.42	0.38	0.41	0.24	0.36	0.39
CaO	4.95	4.33	8.72	9.34	4.93	4.11
Na_2O	6.11	5.34	7.57	6.74	7.07	9.33
K_2O	9.01	7.87	9.00	9.04	9.50	9.84
Total	100.00	100.00	100.00	100.00	100.00	100.00
MgO/(MgO+FeO)	0.47	0.47	0.43	0.44	0.45	0.46
CaO/(CaO+Na_2O)	0.45	0.45	0.54	0.58	0.41	0.31

[1] Average pelite composition of Symmes and Ferry (1991) derived from low grade pelite of Shaw (1956).
[2] Average pelite composition of Mahar et al. (1997).
[3] Average Dalradian subaluminous composition of Atherton and Brotherton (1982).

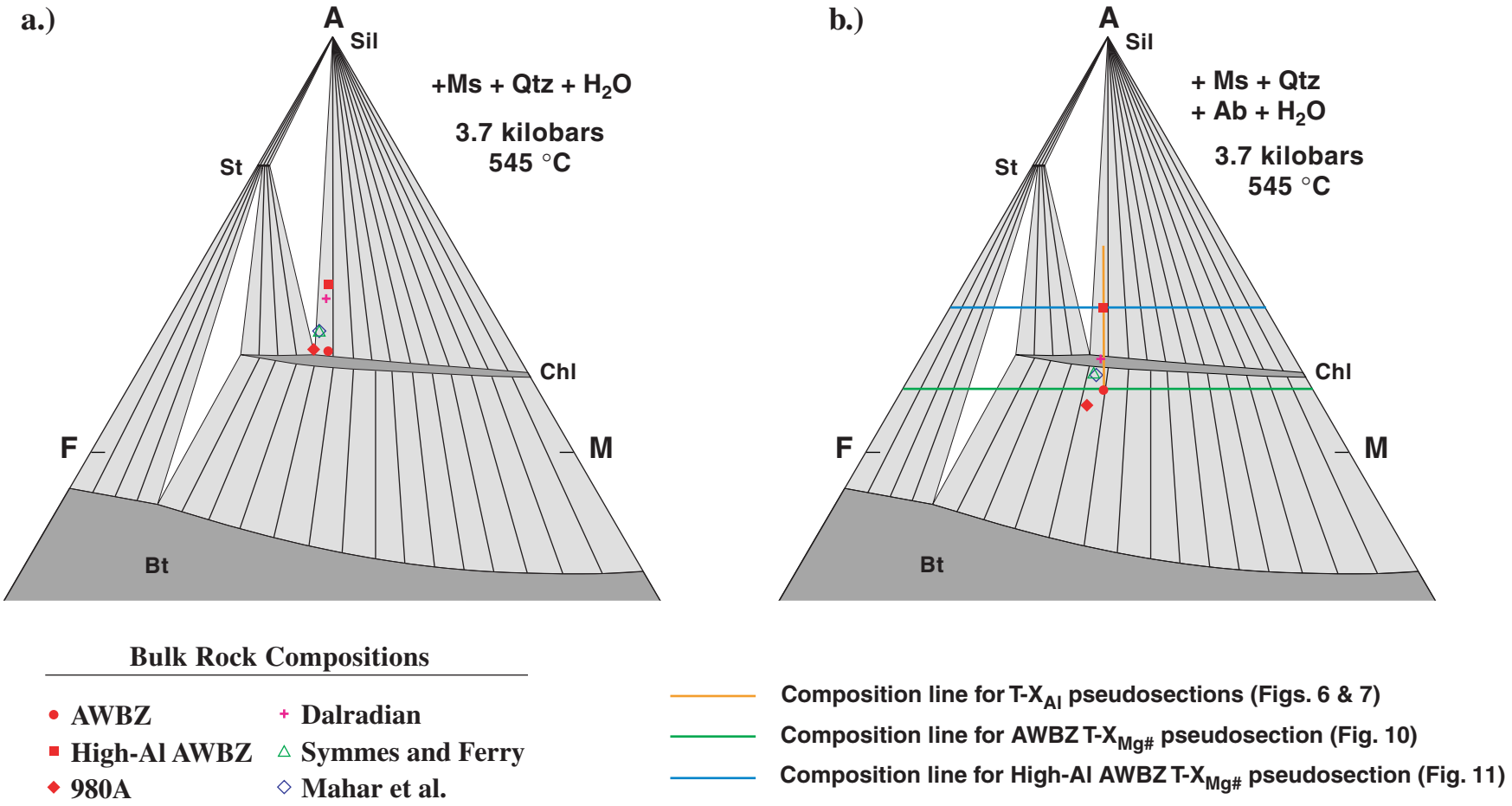

Figure 2. a) AFM projection of bulk rock compositions (projected from Ms, Qtz, and H_2O). b) The same AFM projection as in a, but with the compositions also projected from Ab. Projections calculated at 3.7 kbars, 545 °C. Compositional lines for T-X pseudosections indicated in b.

1977; Spear and Cheney, 1989; Symmes and Ferry, 1992; Droop and Harte, 1995; Mahar et al., 1997; Proyer and Dachs, 2000). This study considers Mn substitution in garnet, staurolite, chloritoid, chlorite, cordierite, and biotite, and Ca substitution in garnet, plagioclase, and to a limited extent, paragonite. The calcic phase zoisite is also considered. Clinozoisite was not considered because the Holland and Powell (1998) dataset predicts zoisite to be more stable than clinozoisite over the P-T range considered in this study. Figures 3 and 4a show KFMASH pseudosections and Figure 5a shows an MnNCKFMASH pseudosection for the AWBZ pelite.

One of the biggest problems with quantitatively modeling pelites with pseudosections in the simplified KFMASH system is deciding how to calculate a KFMASH bulk rock composition equivalent to the real rock composition. Spear (1988, 1999) has shown that natural minerals with non-KFMASH components can be quantitatively projected into the KFMASH system using a set of equilibrium assemblage constraints. This method is not easily applied to bulk rock compositions for pseudosection analysis because it assumes that the prevailing mineral assemblage is known, whereas the assemblage is variable and unknown before constructing the pseudosection. Therefore, assumptions are required when deciding how to project the bulk rock composition into the simplified system.

Assuming the MnNCKFMASH composition as a starting point, one must decided how to eliminate Na_2O, CaO, and MnO to derive the equivalent KFMASH composition. The MnO and CaO components are difficult because minerals in addition to garnet may contain substantial amounts of Mn, and in the MnNCKFMASH component system, garnet, zoisite, and plagioclase may contain substantial amounts of Ca. Simply removing CaO and the Al_2O_3 and SiO_2 associated with anorthite, grossular, and zoisite is not appropriate, as the modal abundance and/or equilibrium composition of plagioclase, garnet, and zoisite are different at each P-T point in the pseudosection. As a result, the formula needed to quantitatively remove the CaO component is different for each P-T value. Therefore, we have simply eliminated MnO and CaO (leaving Al_2O_3 and SiO_2 unchanged), leaving Na_2O as the only non-KFMASH component. In the paragonite-free portion of P-T space, Na will predominantly enter the plagioclase structure, with only minor amounts substituting into muscovite. Therefore, it is reasonable to eliminate Na_2O from the composition by assuming all Na substitutes into plagioclase and removing the associated Al_2O_3 and SiO_2 (projecting from albite). Figure 3 shows a KFMASH pseudosection for a composition derived by simply subtracting Na_2O from the NKFMASH composition, and Figure 4a shows the corresponding KFMASH pseudosection derived by projection from albite. The plotting positions for these two compositions are shown on an AFM ternary projection in Figures 2a and 2b. Since both pseudosections were constructed with quartz in excess, the only effective difference between the two KFMASH compositions is the relative proportion of Al_2O_3. The effect of not projecting from albite results in a bulk composition higher in Al. This results in a substantial increase in predicted stability of staurolite, aluminum silicate, and chloritoid for the AWBZ (compare Figs. 3 and 4a). Chloritoid, which is not predicted as a stable phase anywhere in the P-T window of interest when projecting the composition from albite, has a significant stability field at pressures above 6 kbars for the composition with higher Al content. Chloritoid, staurolite, and aluminum silicate are predicted to join the assemblage at lower temperatures than biotite for the composition not projected from albite. Projecting the AWBZ from albite results in a low-Al pelite whereas simply eliminating Na from the AWBZ results in a high-Al pelite . Clearly , the method of deriving a KFMASH composition has a significant effect on predicted assemblage stability for pelitic rocks and must be considered when comparing KFMASH pseudosections to natural rocks.

Comparison of KFMASH and MnNCKFMASH

The method of removing MnO and CaO from the rock composition plays an important role in predicted mineral assemblage stability. There is no ideal method for subtracting MnO and CaO for the purpose of modeling natural rocks with pseudosections; therefore, we submit that it is more appropriate to use the MnNCKFMASH system than the KFMASH, MnKFMASH, or NCKFMASH systems. Comparing the MnNCKFMASH AWBZ pseudosection (Fig. 5) with the KFMASH pseudosections highlights the combined effect of adding the MnO, Na_2O, and CaO components. Because we believe that projecting the composition from albite produces a KFMASH pseudosection that is more comparable to MnNCKFMASH pseudosections than the one not projected from albite, all subsequent comparisons are made to this KFMASH pseudosection (Fig. 4a) only. The stability of those minerals that appear in both systems is discussed first, followed by a discussion of non-KFMASH phase stability.

Biotite is stabilized to lower temperatures in the MnNCKFMASH system than in the KFMASH system. The AWBZ pseudosection (Fig. 5b) predicts the biotite-in isograd at 420 °C at 3.5 kbars, in good agreement with 400 °C calculated by Ferry (1984) for the Waterville Fm.

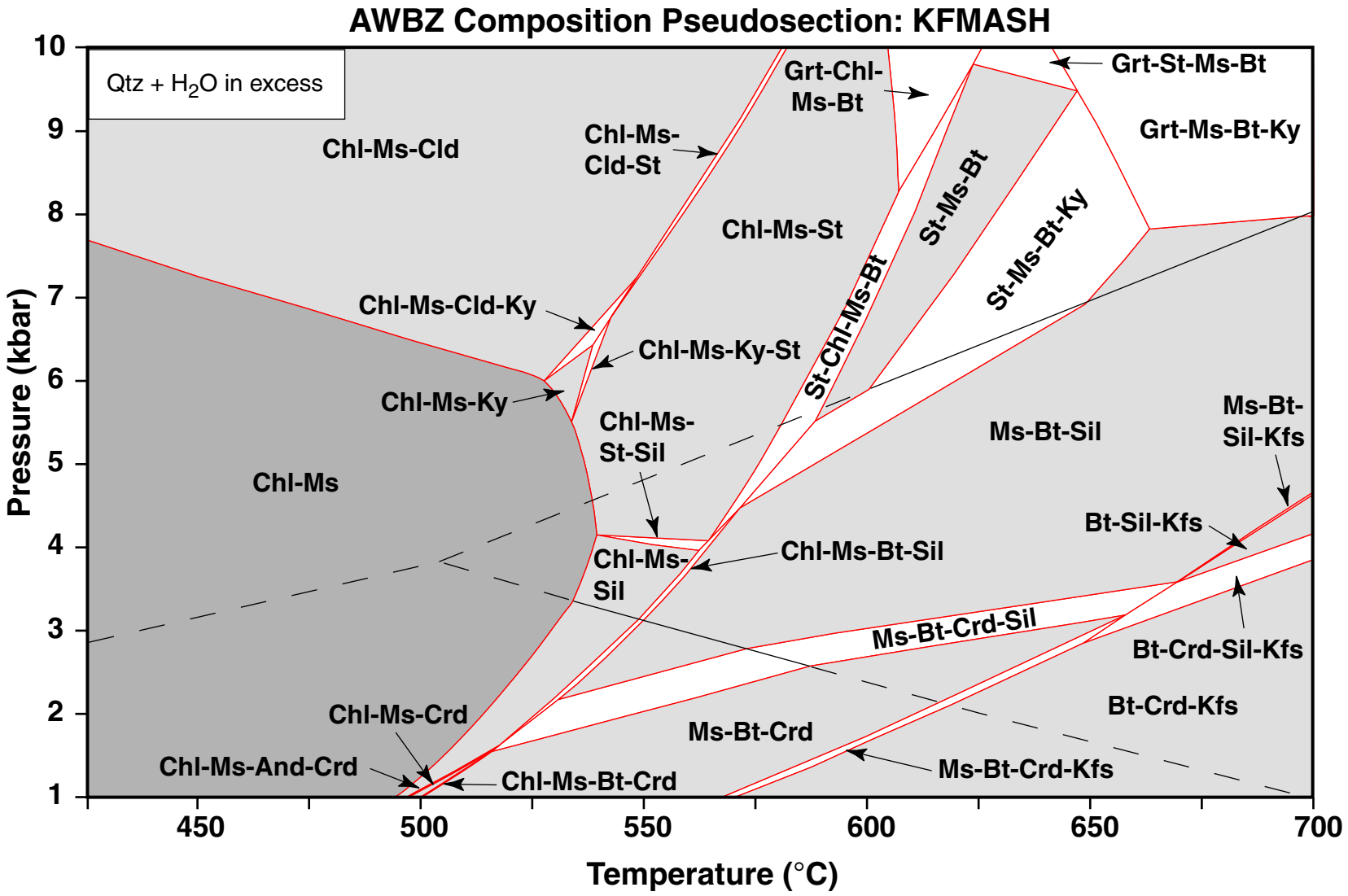

Figure 3. KFMASH pseudosection for the AWBZ composition with Na_2O, MnO, and CaO subtracted (see text; composition plotted in Fig. 2a). Aluminum silicate triple point shown for reference.

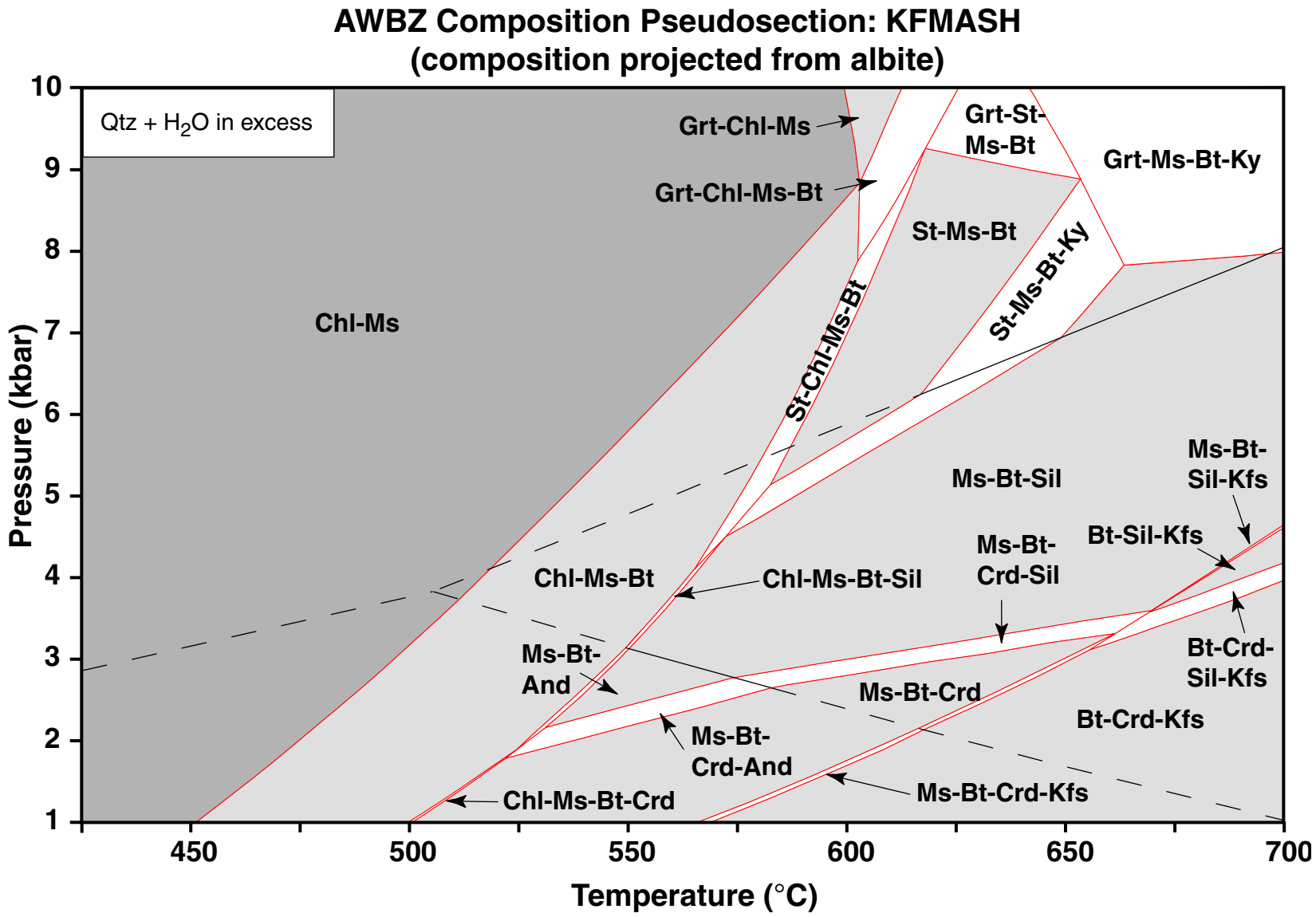

Figure 4a. KFMASH pseudosection for the AWBZ composition modified by subtracting MnO and CaO, and projecting from Ab (see text; composition plotted in Fig. 2b). Aluminum silicate triple point shown for reference.

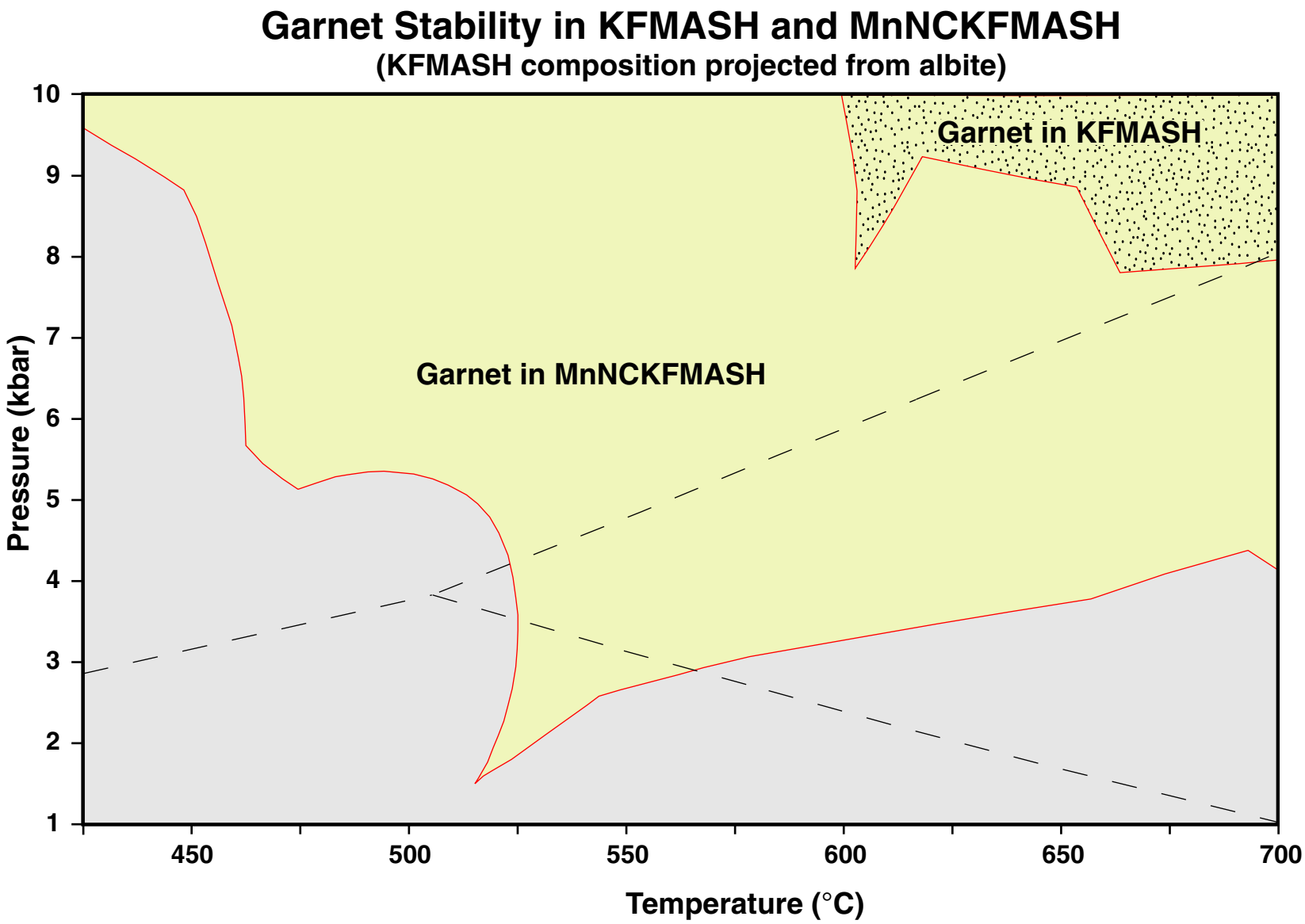

Figure 4b. Comparison of garnet stability in the systems KFMASH (Fig. 4a) and MnNCKFMASH for the AWBZ composition. Aluminum silicate triple point shown for reference.

In contrast, the KFMASH pseudosection predicts the biotite-in isograd at approximately 510 °C at 3.5 kbars. Ferry (1984) shows that the biotite isograd separates carbonate bearing chlorite zone rocks from biotite zone and higher grade carbonate free rocks. This was interpreted as a decarbonation front that was driven by H_2O fluid infiltration. Ferry (1984) indicates metamorphic fluid in the Waterville Fm. approaches that of a binary CO_2-H_2O fluid with a small fraction of CO_2 (X_{CO_2} = 0.02 - 0.04) at the biotite isograd. In addition, Waterville Fm. pelites in the chlorite zone contain albite, whereas they contain oligoclase in the biotite zone (Ferry, 1984). This study does not consider carbonate minerals or binary CO_2-H_2O fluid, nor does it consider a pure albite phase, and therefore the AWBZ pseudosection presented here is likely not relevant below the biotite isograd at the P-T conditions of Waterville Fm. metamorphism. Therefore, it is likely that the biotite forming reaction predicted by the pseudosection is not the same as that which produced biotite in the Waterville Fm., but the lack of carbonate and presence of calcic plagioclase above the biotite isograd indicate that exclusion of carbonate and pure albite is not a problem above the biotite isograd.

Previous studies indicate that Mn stabilizes garnet to substantially lower temperatures and pressures in the MnNCKFMASH system relative to KFMASH (Trzcienski, 1977; Spear and Cheney, 1989; Mahar et al., 1997; Symmes and Ferry, 1992). The stability of garnet in the two systems is compared in Fig. 4b, which clearly show that addition of Mn and Ca to the KFMASH system has a tremendous affect on garnet stability. The KFMASH pseudosection predicts garnet to be stable only at temperatures and pressures above approximately 600 °C and 7 kbars, whereas the stability field of garnet in the AWBZ MnNCKFMASH pseudosection is considerably enlarged. In the MnNCKFMASH system, garnet is unstable at low pressures, and generally becomes less stable with increasing temperature up to 687 °C, where it is stabilized to lower pressures with increasing temperature after sillimanite reacts out of the assemblage. The lowest pressure limit of garnet stability across the pseudosection is about 1.5 kbars near 515 °C. In the common assemblage Grt-Chl-Ms-Bt-Pl, the garnet-in isopleth sweeps to increasing temperature up pressure in the interval 1.5 - 3.0 kbars. Above 3.0 kbars, the garnet-in isopleth sweeps to lower temperature with increasing pressure, down to approximately 425 °C at 9.5 kbars. Although the AWBZ is slightly enriched in MnO relative to other common pelite compositions (Table 1), garnet is predicted to be unstable at the aluminum-silicate triple point of the Holland and Powell (1998) data set (3.8 kbars, 505 °C). The extreme temperature dependence of the garnet-in isopleth on MnO content was clearly illustrated by Mahar et al. (1997, their Fig. 5), and we predict that with MnO contents slightly above that in AWBZ (e.g., 980A, discussed below), garnet would be stabilized to temperatures below the triple point. The widespread occurrence of garnet in the Waterville Fm. samples (Ferry, 1982) metamorphosed at approximately 3-4 kbars clearly indicates KFMASH is not appropriate for considering garnet stability in these samples.

Cordierite is restricted to low pressures and temperatures above 500 °C (Fig. 5f). Cordierite stability in KFMASH is very similar to that predicted in MnNCKFMASH. Therefore, the only other significant difference in KFMASH bearing mineral stability between the two systems is that of staurolite. Staurolite has a very restricted P-T stability field in MnNCKFMASH, confined to the interval 575-630 °C and 4-8 kbars (Fig. 5c). Staurolite is stabilized to slightly higher pressures and lower temperatures in the KFMASH system, which likely reflects the effective difference in Al content in the two systems. The presence of non-KFMASH Al-bearing phases, and phases stabilized by Mn more than staurolite, essentially depletes the amount of Al available to staurolite (which is stabilized by increased Al in the KFMASH system).

Addition of Na_2O and CaO allows modeling of plagioclase, paragonite, and zoisite/clinozoisite stability. In addition, inclusion of CaO allows calculation of the grossular component of garnet. Margarite was not considered in this study, so the results shown here do not apply to margarite bearing rocks. The AWBZ pseudosection predicts zoisite as a stable phase at and just above the biotite isograd. Zoisite has not been reported as a typical phase in biotite zone pelitic rocks of the Waterville Fm., but clinozoisite is occasionally observed in the garnet, staurolite-andalusite, and sillimanite zones (Ferry, 1982). The lack of predicted zoisite occurrence above the biotite zone below 5 kbars is at odds with the occurrence of clinozoisite reported by Ferry (1982). For the Holland and Powell (1998) data set, zoisite is more stable than clinozoisite at the temperatures of interest here, and replacement of zoisite by clinozoisite for modeling purposes does not alleviate the discrepancy. However, Waterville Fm. samples have significant variation in CaO content, indicating that the AWBZ Ca content used here may not be adequate for modeling some Waterville Fm. samples. Since epidote cannot be modeled in the MnNCKFMASH system, we have not evaluated the effect of Fe^{3+}, which could stabilize epidote group minerals to higher temperatures. Regardless of the discrepancies at low pressures, at higher pressures the pseudosection predicts garnet growth before zoisite reacts out with increased temperature and a

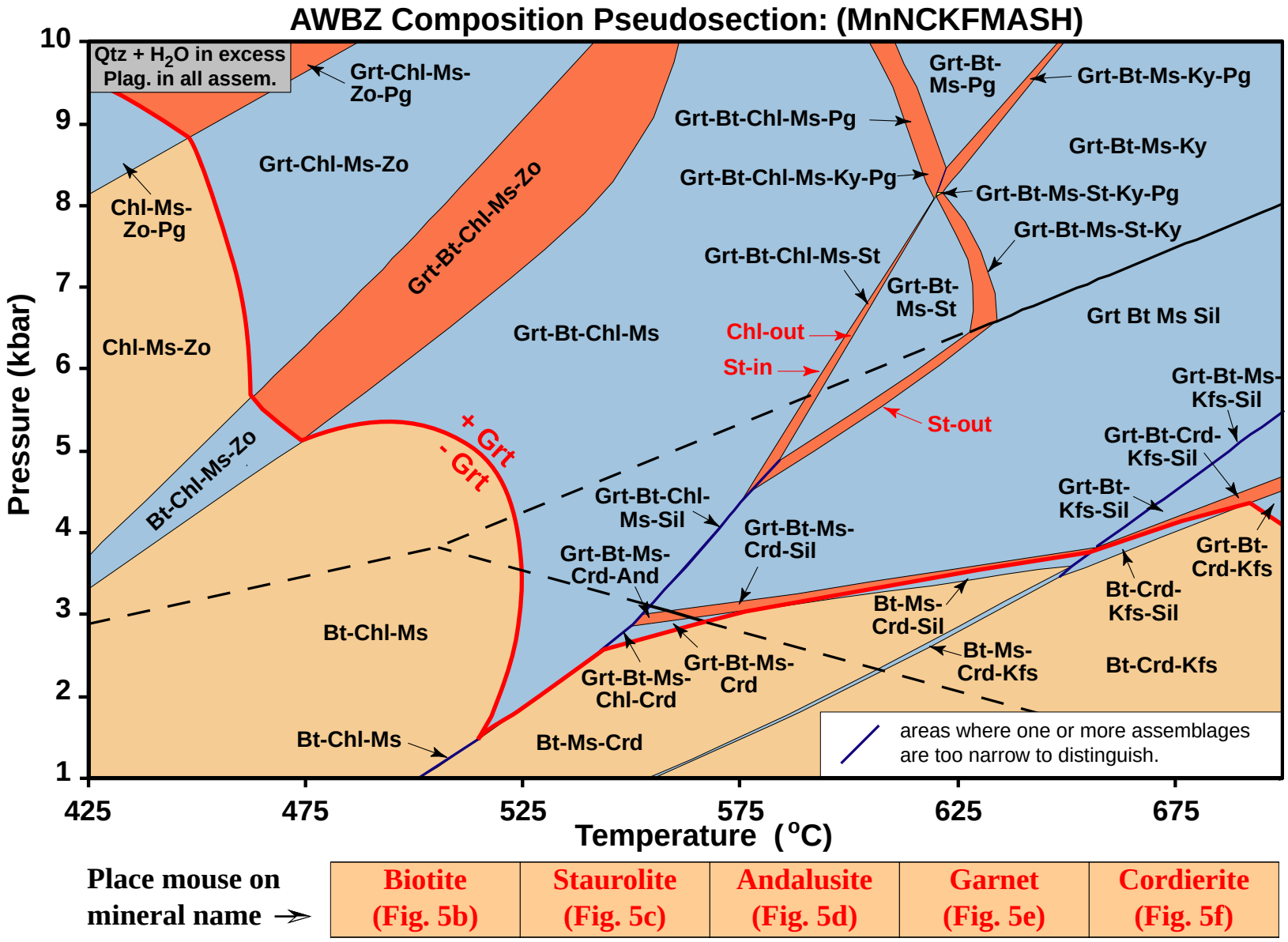

Place mouse on mineral name →	Biotite (Fig. 5b)	Staurolite (Fig. 5c)	Andalusite (Fig. 5d)	Garnet (Fig. 5e)	Cordierite (Fig. 5f)

Figure 5a. MnNCKFMASH pseudosection for the average Waterville biotite zone composition (AWBZ).

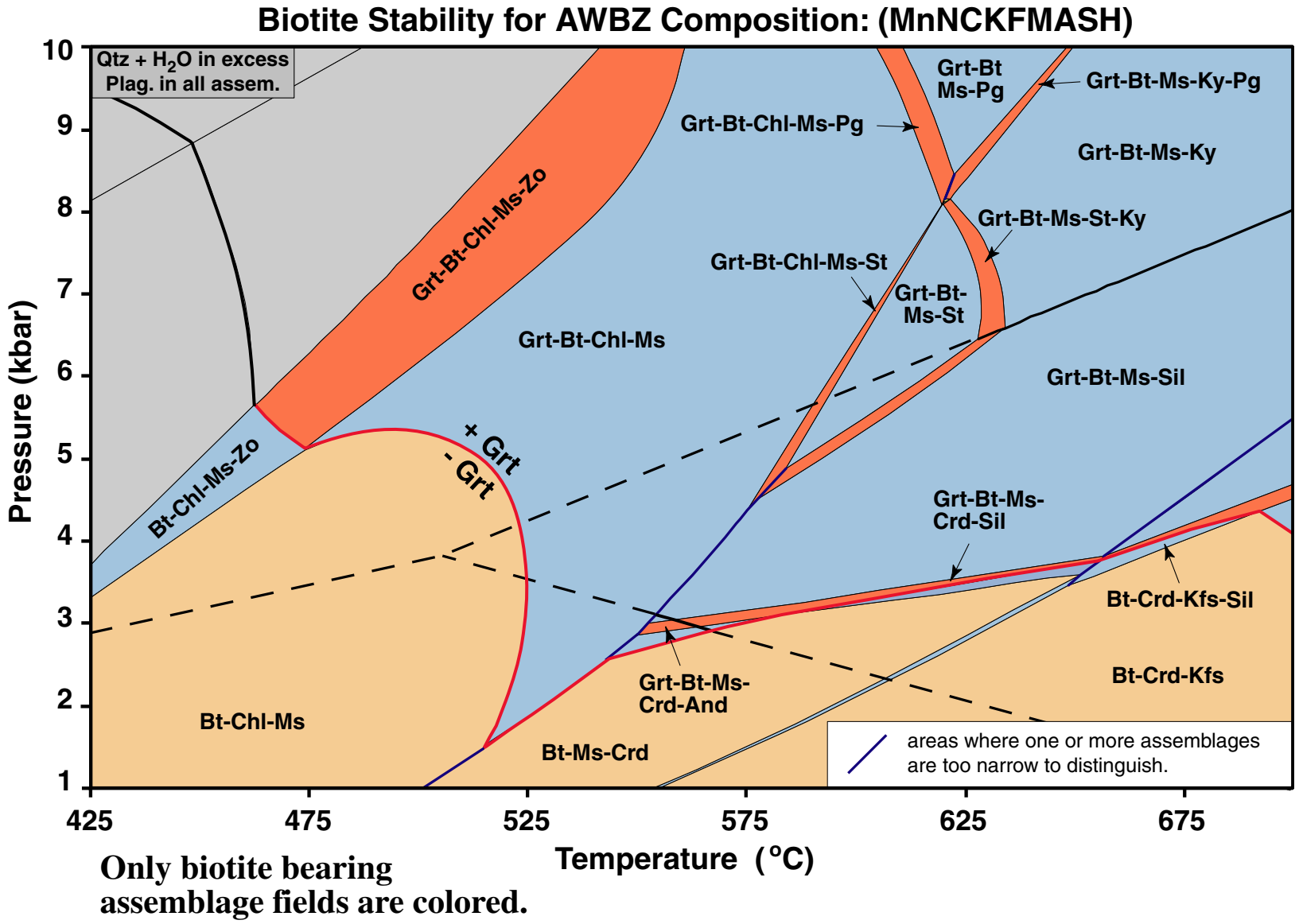

Figure 5b. Biotite stability (in color) for the AWBZ composition.

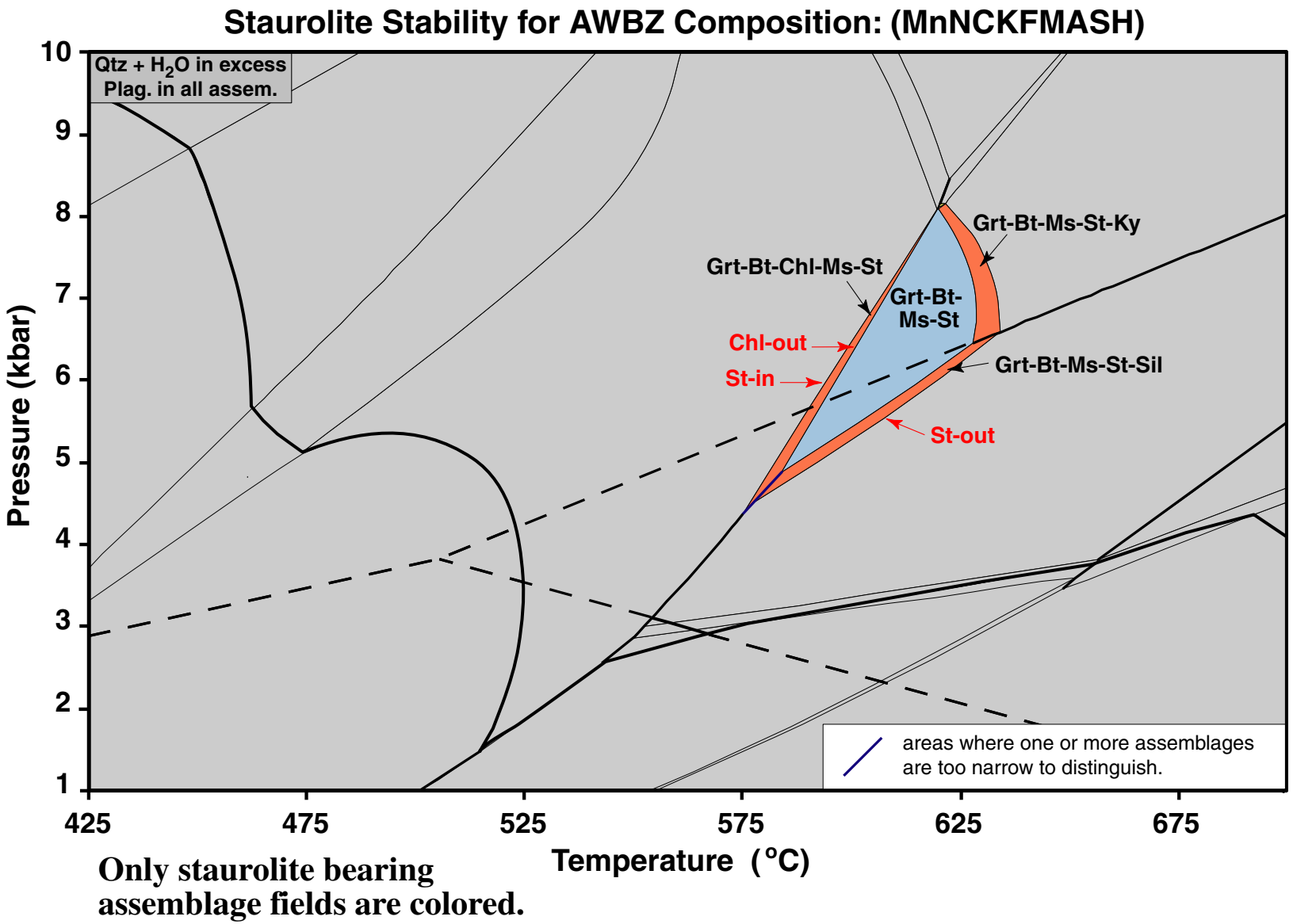

Figure 5c. Staurolite stability (in color) for the AWBZ composition.

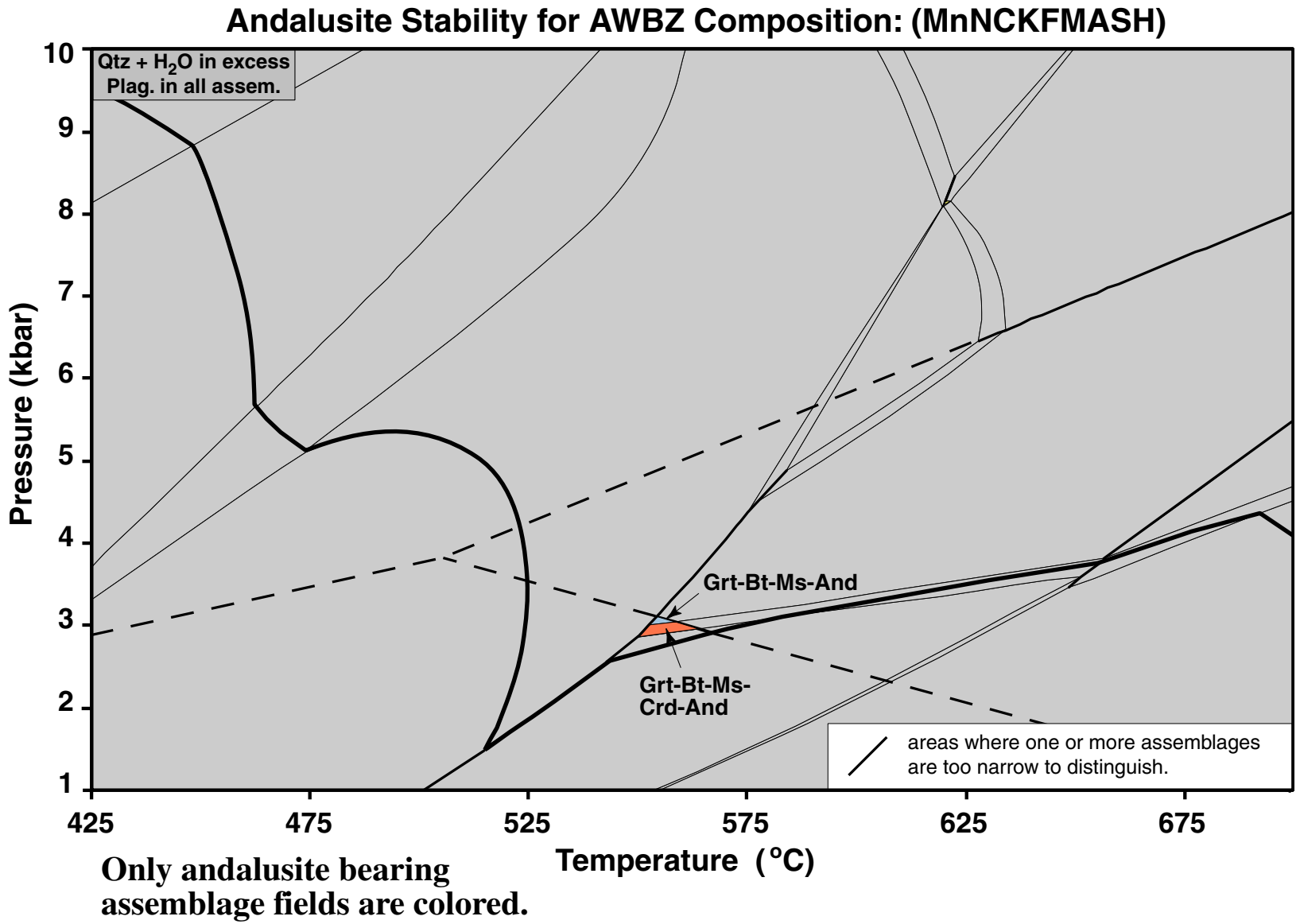

Figure 5d. Andalusite stability (in color) for the AWBZ composition.

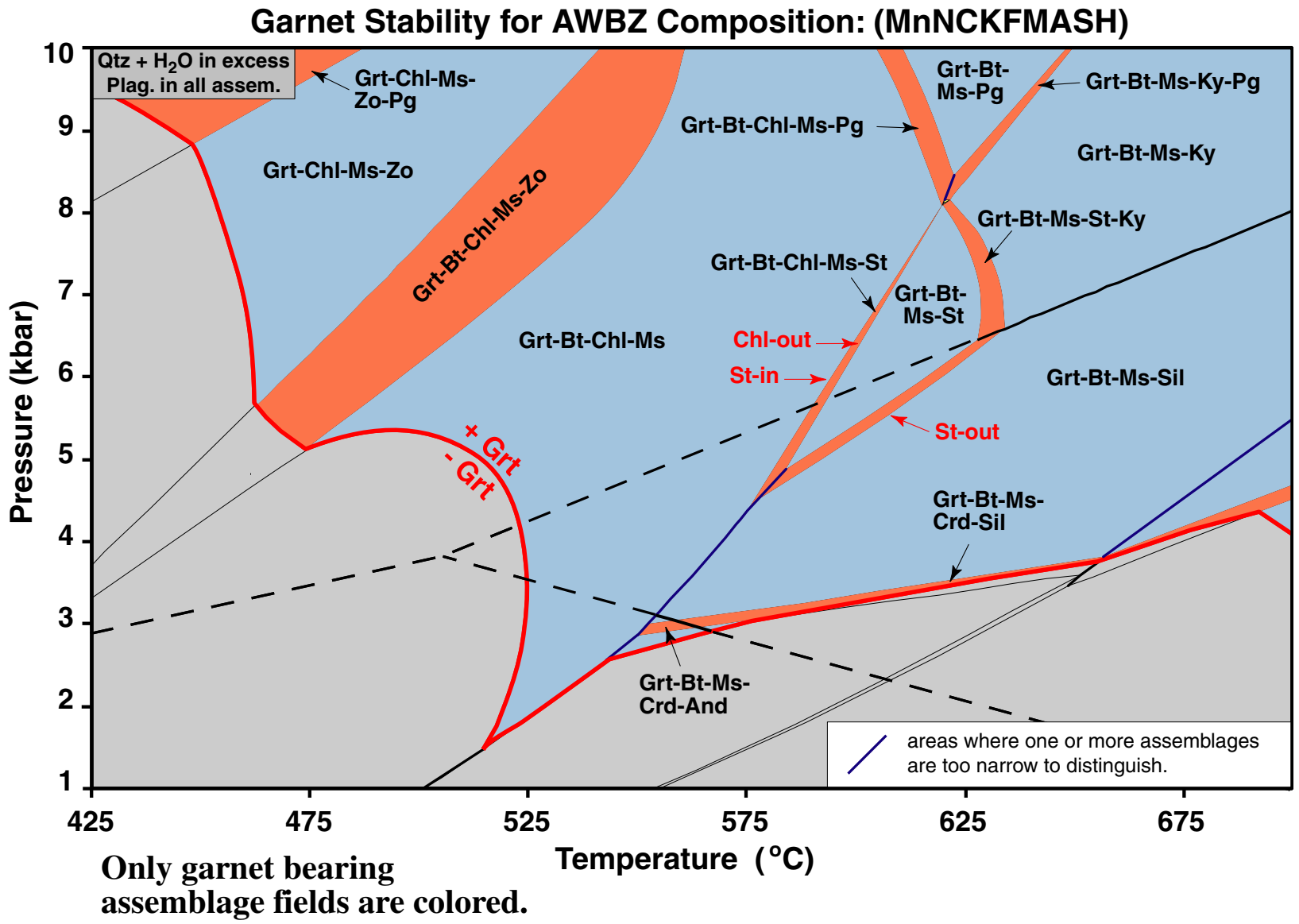

Figure 5e. Garnet stability (in color) for the AWBZ composition.

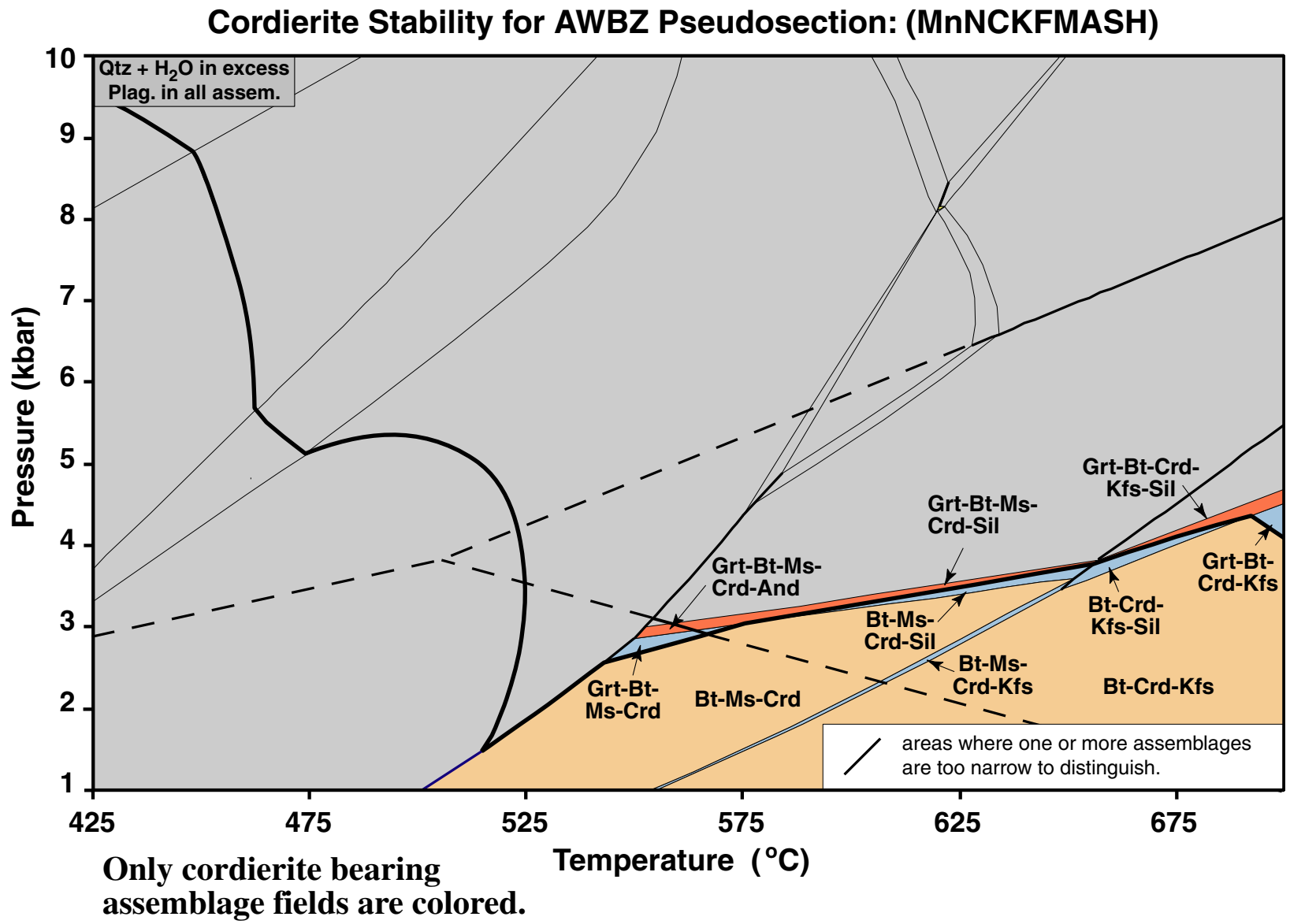

Figure 5f. Cordierite stability (in color) for the AWBZ composition.

positive slope for zoisite-out reactions, both of which agree with observations from natural rocks (Menard and Spear, 1993; Stowell et al., 1996).

Plagioclase is predicted to be stable throughout the P-T window considered in this study. Paragonite is stable at pressures > 8 kbars at temperatures < 500 °C and in the interval 600 to 650 °C. Both plagioclase and paragonite stability change significantly with increased Al and Ca content (discussed below). Andalusite has a very restricted stability field (< 3 kbars, ≈550 °C; Fig. 5d), sillimanite is only stable above 550 °C, and kyanite is only stable above ≈620 °C. Therefore, aluminum silicate is not stable at the triple point, consistent with the arguments of Pattison (2001) that aluminum silicates are not stable at the triple point in low-Al pelites.

Effect of Bulk Rock Composition

A series of T-X pseudosections is presented for variable Al content and Mg# to address the effect of bulk rock composition on assemblage stability. T-X pseudosections are ideal for isolating the effect of a single component or the effect of a compositional ratio because they show the continuous variability in mineral assemblage stability as the composition changes along a compositional vector (at constant pressure). P-X pseudosections, though useful for showing changes with pressure at constant temperature, are not presented here because the suite of Waterville Fm. samples considered in this study likely experienced metamorphism over a relatively small range of pressures. In addition to the T-X pseudosections, two additional P-T pseudosections are shown, one corresponding to the AWBZ with an increased Al content, and one for a staurolite-andalusite zone sample composition (sample 980A). The compositional ranges for the T-X pseudosections are indicated on an AFM projection in Figure 2b.

Effect of Al_2O_3 content

T-X_{Al} pseudosections, at 3.5 and 5 kbars, are shown in Figures 6 and 7, respectively. In both, the AWBZ plots at 37.99 mole % Al_2O_3, and 51.00 mole % Al_2O_3 corresponds to a very aluminous AWBZ (Fig. 2).

T-X_{Al} pseudosection, 3.5 kbars (Fig. 6). The T-X_{Al} pseudosection at 3.5 kbars shows that Al content plays an important role in Bt, Sil/And, and Pg stability below 560 °C. With increasing Al content, biotite is destabilized and sillimanite is stabilized to lower temperatures. At 44.3% Al_2O_3 and 561 °C, the following assemblages meet: Grt-Chl-Ms-Bt-Pl-Qtz-H_2O, Grt-Chl-Ms-Pl-Qtz-H_2O, Grt-Chl-Ms-Pl-Sil-Qtz-H_2O, and Grt-Chl-Ms-Bt-Pl-Sil-Qtz-H_2O. Above 561 °C, the trivariant assemblage Grt-Chl-Ms-Bt-Pl-Sil-Qtz-H_2O is stable across the pseudosection over a 2 degree interval. This trivariant assemblage at 561-563 °C is essentially equivalent to the kyanite bearing univariant KFMASH reaction

$$Grt + Chl + Ms = Bt + Ky + Qtz + H_2O$$

This KFMASH univariant is only stable above 11 kbars (within the kyanite field); therefore, this sillimanite bearing MnNCKFMASH assemblage cannot occur in KFMASH. This is a rather important point when comparing chemically complex rocks to simplified chemical system modeling. Univariant reactions in a simplified chemical system become higher variance assemblage fields in more complex systems. At temperatures below 561 °C, 44.3% Al_2O_3 separates the assemblage Grt-Chl-Bt-Ms-Pl-Qtz-H_2O at low Al_2O_3 from the assemblage Grt-Chl-Sil-Ms-Pl-Qtz-H_2O at higher Al_2O_3, and marks the transition from low-Al pelite to high-Al pelite in terms of mineral assemblages.

Sillimanite stability increases to lower temperatures with increased Al above 44.3% Al_2O_3. This trend results in andalusite stability above 48% Al_2O_3. Below 530 °C and below 46% Al_2O_3, paragonite is stabilized to higher temperatures with increasing Al until it coexists with sillimanite. With sillimanite in the assemblage, the upper temperature limit of paragonite stability becomes nearly independent of Al content, as indicated by the horizontal paragonite-out isopleth going from Chl-Ms-Pl-Pg-Sil-Qtz-H_2O to Chl-Ms-Pl-Sil-Qtz-H_2O with increasing temperature. In the presence of paragonite, aluminum-silicate stability extends to lower temperatures with increased Al due to Ca-Na solid solution in plagioclase and paragonite (both plagioclase and paragonite become enriched in Ca with a decrease in temperature, requiring higher bulk rock Al for aluminum-silicate stability). Paragonite plays an important role in aluminum silicate stability. If paragonite were not considered in construction of this pseudosection, the sillimanite-in boundary between the assemblages Chl-Ms-Pl-Qtz-H_2O and Chl-Ms-Pl-Sil-Qtz-H_2O (at Al_2O_3 > 46%) would extend with increased Al to even lower temperatures than the sillimanite- and andalusite-in boundaries in the paragonite bearing assemblages. This leads to aluminum silicate stability at lower Al than when paragonite is present. If paragonite were absent, increased Al would eventually lead to kyanite stability below 479 °C at Al_2O_3 > 50%. Therefore, the presence of paragonite clearly plays an important role in predicted andalusite and kyanite stability at temperatures below 525 °C along this compositional line.

Garnet is relatively unaffected by Al content at 3.5 kbars. The lower temperature limit of garnet stability increases by only 10° between 38% Al_2O_3 and 51%

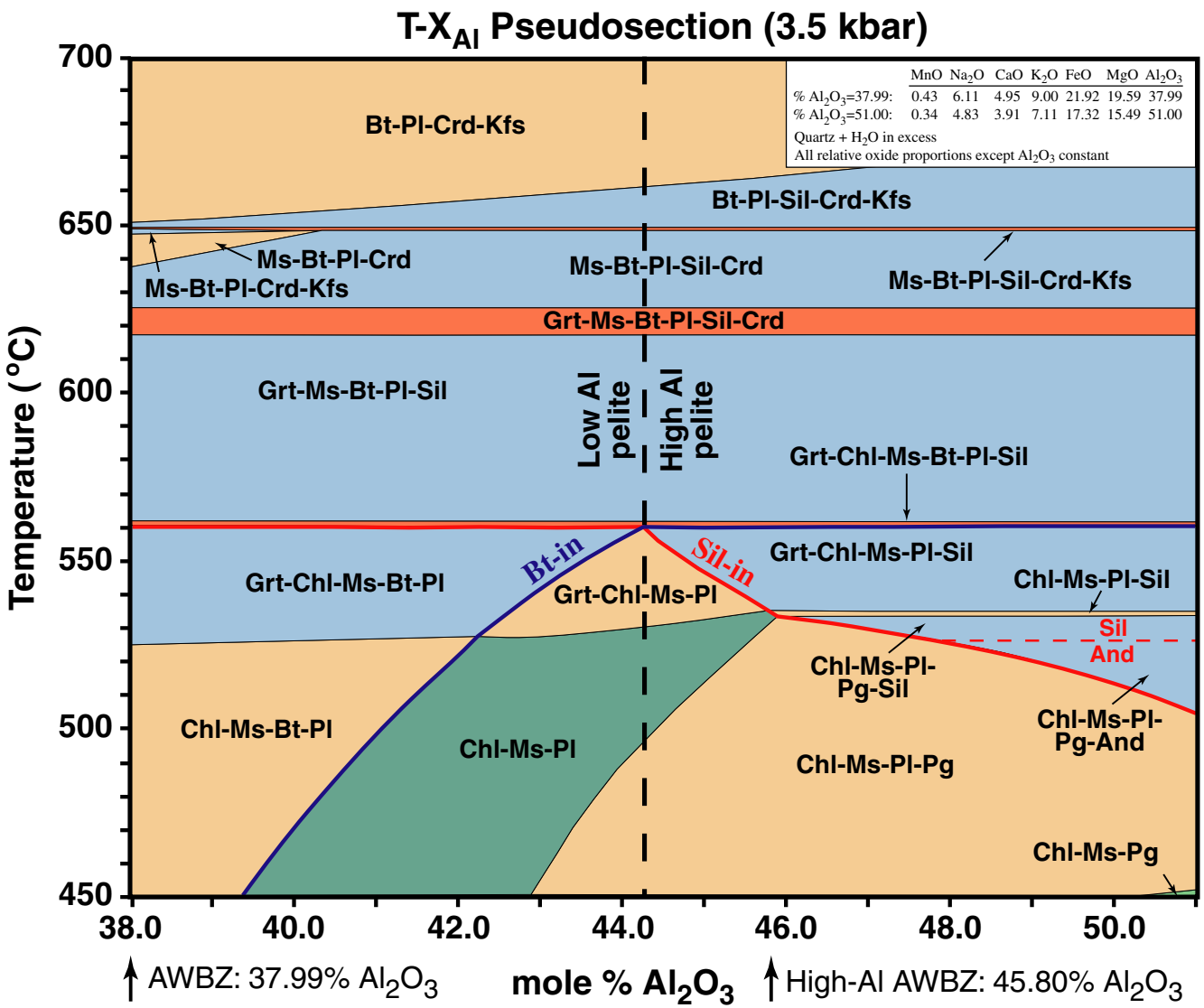

Figure 6. T-X_{Al} pseudosection at 3.5 kbars, from the AWBZ composition at 37.99% Al_2O_3 to 51.00% Al_2O_3 (mole % based on SiO_2- and H_2O- free compositions). The High-Al AWBZ pseudosection composition (Fig. 8) has 45.80% Al_2O_3.

Al_2O_3. In the interval 561-700 °C, mineral stability is relatively unaffected by Al content for the compositions considered here. This is shown by the horizontal zero mode isopleths for chlorite, garnet, cordierite, muscovite, and K-feldspar. Sillimanite is the only phase that shows stability dependence on Al content above 561 °C, where it is stabilized to slightly higher temperatures with increased Al. Although one might expect chloritoid as a stable phase at high bulk rock Al, chloritoid does not appear in this pseudosection because of the bulk rock MgO/(MgO+FeO) (discussed in more detail below).

T-X_{Al} pseudosection, 5 kbars (Fig. 7). The T-X_{Al} pseudosection at 5 kbars is more complicated than the one at 3.5 kbars due to the additional stability of staurolite, chloritoid, and zoisite. The stability of staurolite, chloritoid, and zoisite are all strongly dependent on Al. Staurolite is stabilized to lower temperatures with increasing Al content. The transition from low-Al pelite to high-Al pelite at 5 kbars is defined by the stability of staurolite and biotite. Below 581 °C, 43.7% Al_2O_3 separates the paragenesis Grt-Chl-Bt at low Al_2O_3 from Grt-Chl-St at high Al_2O_3. Just above 581 °C, the paragenesis Grt-Chl-Bt-St is stable for approximately 4 degrees, and is equivalent to the KFMASH Grt-Chl tie line breaking reaction

$$Grt + Chl + Ms = St + Bt + Qtz + H_2O.$$

This KFMASH reaction occurs at 559 °C at 5 kbars, approximately 20 degrees lower than the equivalent MnNCKFMASH paragenesis. Therefore, it is concluded that the high-Al/low-Al boundary is slightly pressure dependent.

Zoisite is stable at low temperatures in the 5 kilobar T-X_{Al} pseudosection, and is destabilized at higher temperatures with increasing Al until paragonite joins the assemblage. With paragonite in the assemblage, zoisite is stabilized to higher temperatures with increasing Al content. This is likely due to the destabilization of plagioclase with increasing Al content when paragonite and zoisite are present. Chloritoid is only stable above 50% Al_2O_3 in this pseudosection, with its stability field increasing to lower temperatures with increased Al content.

High-Al AWBZ P-T pseudosection (Fig. 8). A P-T pseudosection for the High-Al AWBZ, calculated by increasing Al_2O_3 and decreasing all other oxides (including MnO) proportionally, is shown in Figure 8. This composition plots at 45.8% Al_2O_3 in the T-X_{Al} pseudosections and corresponds to a high-Al pelite (Fig. 2b). The proportional decrease in MnO content decreases garnet stability at low temperatures. The higher Al content leads to a substantial increase in paragonite, staurolite, and aluminum silicate stability (Fig. 9). The andalusite stability field is substantially increased at low pressures by the stability of the Pl-Ms-Chl-And-Qtz-H_2O assemblage. This assemblage forms by conversion of aluminum-rich chlorite to aluminum-poor chlorite and conversion of the paragonite component of muscovite to albite with increasing temperature and decreasing pressure. Staurolite stability is increased to lower temperatures (down to 543 °C) with only an insignificant increase to lower pressures (4 kbars). Paragonite is stabilized to < 1 kilobar at 425 °C and up to 648 °C at 10 kbars. Sillimanite and andalusite are stabilized to lower pressures and slightly lower temperatures. Compared to the AWBZ pseudosection, plagioclase stability is decreased at higher pressures below 575 °C.

Effect of Mg/(Fe+Mg)

The effect of variable Mg# (MgO/(MgO+FeO)) on assemblage stability is shown in two T-$X_{Mg\#}$ pseudosections. One pseudosection corresponds to the AWBZ (Fig. 10), and the other to the High-Al AWBZ (Fig. 11). In both, $X_{Mg\#} = 0$ corresponds to a composition with the mole proportion of MgO set to zero and mole proportion of FeO set to the sum of FeO and MgO in the bulk rock composition, and $X_{Mg\#} = 1$ corresponds to a composition with mole proportion of FeO set to zero and mole proportion of MgO set to the sum of FeO and MgO in the bulk rock composition.

T-$X_{Mg\#}$ pseudosection for the AWBZ (Fig. 10). The T-$X_{Mg\#}$ pseudosection shows that garnet, cordierite, sillimanite, and staurolite stability are strongly dependent on $X_{Mg\#}$. Garnet stability is restricted to $X_{Mg\#} < 0.68$, and extends down to 428 °C at $X_{Mg\#} = 0$. Staurolite stability is restricted to the range $X_{Mg\#} = 0.1$ to $X_{Mg\#} = 0.4$ at approximately 540-580 °C. The lowest temperature stability of cordierite is approximately 560 °C at $X_{Mg\#} > 0.6$, but extends to $X_{Mg\#} < 0.1$ at higher temperatures (690 °C). Sillimanite stability is restricted to $X_{Mg\#} < 0.62$ and temperatures higher than 555 °C. Chloritoid is not predicted as a stable phase at moderate temperatures, consistent with the interpretation that this composition corresponds to a low-Al pelite, but is also absent at low temperatures. The reason chloritoid is not predicted at low $X_{Mg\#}$ and low temperatures is likely due to the effect of Mn on stabilization of garnet at low temperatures to stabilize the paragenesis Grt + Chl (Spear, 1993, pg. 354).

Muscovite and potassium feldspar coexist over a small temperature interval due to solid solution in both phases. The pseudosection clearly shows the temperature

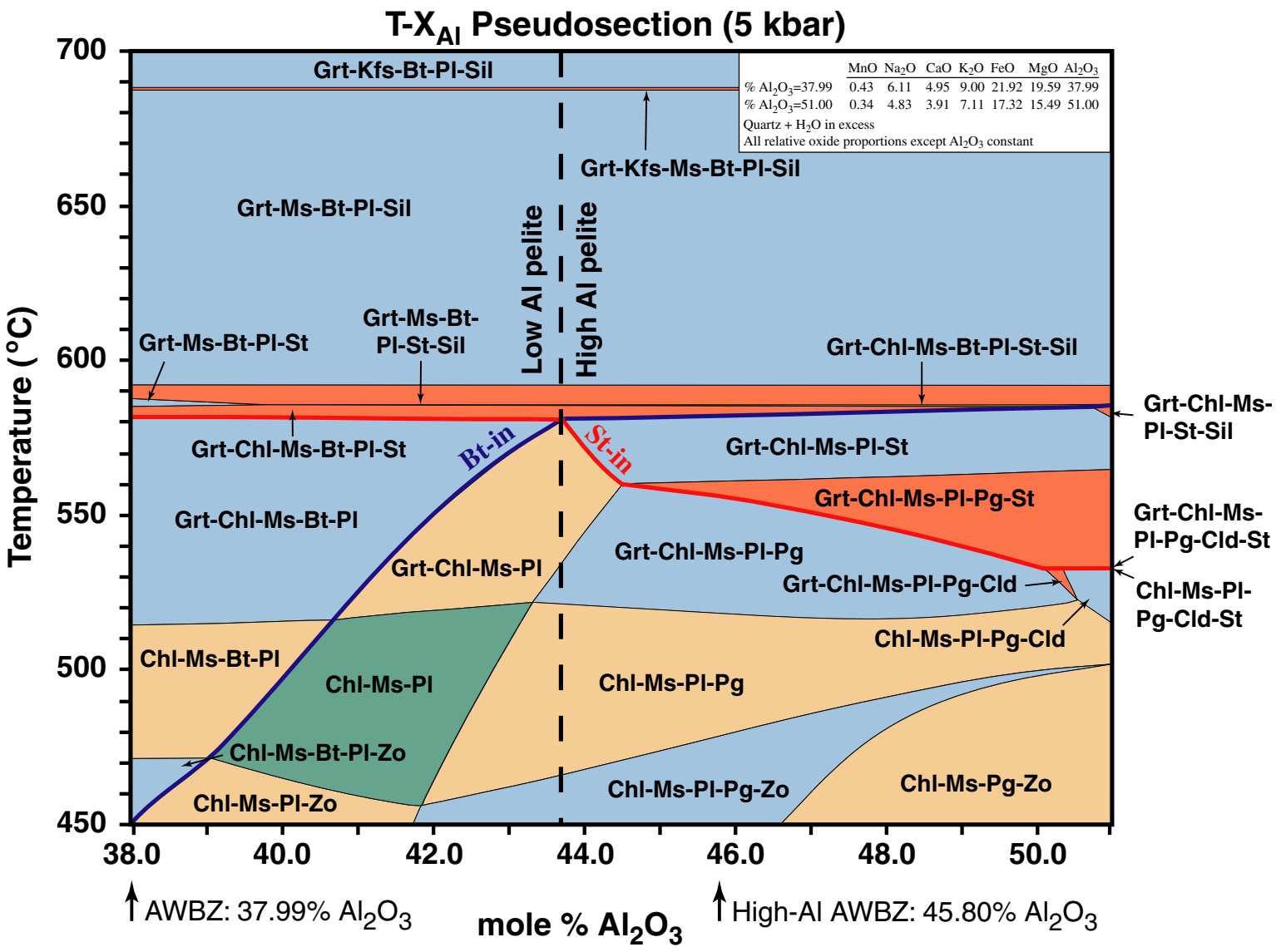

Figure 7. T-X_{Al} pseudosection at 5 kbars, from the AWBZ composition at 37.99% Al_2O_3 to 51.00% Al_2O_3 (mole % based on SiO_2- and H_2O- free compositions). The High-Al AWBZ pseudosection composition (Fig. 8) has 45.80% Al_2O_3.

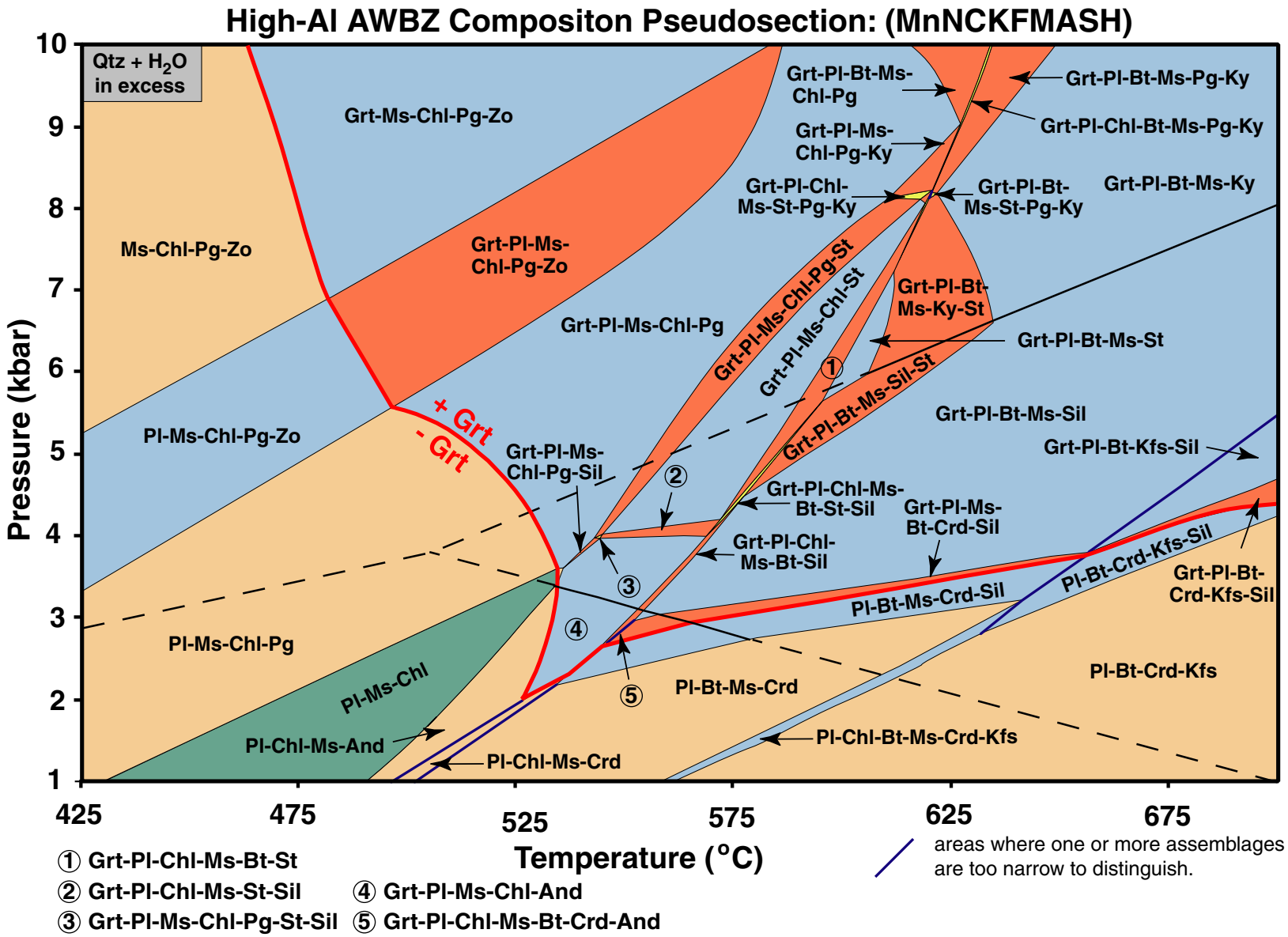

Figure 8. MnNCKFMASH P-T pseudosection for the High-Al AWBZ composition.

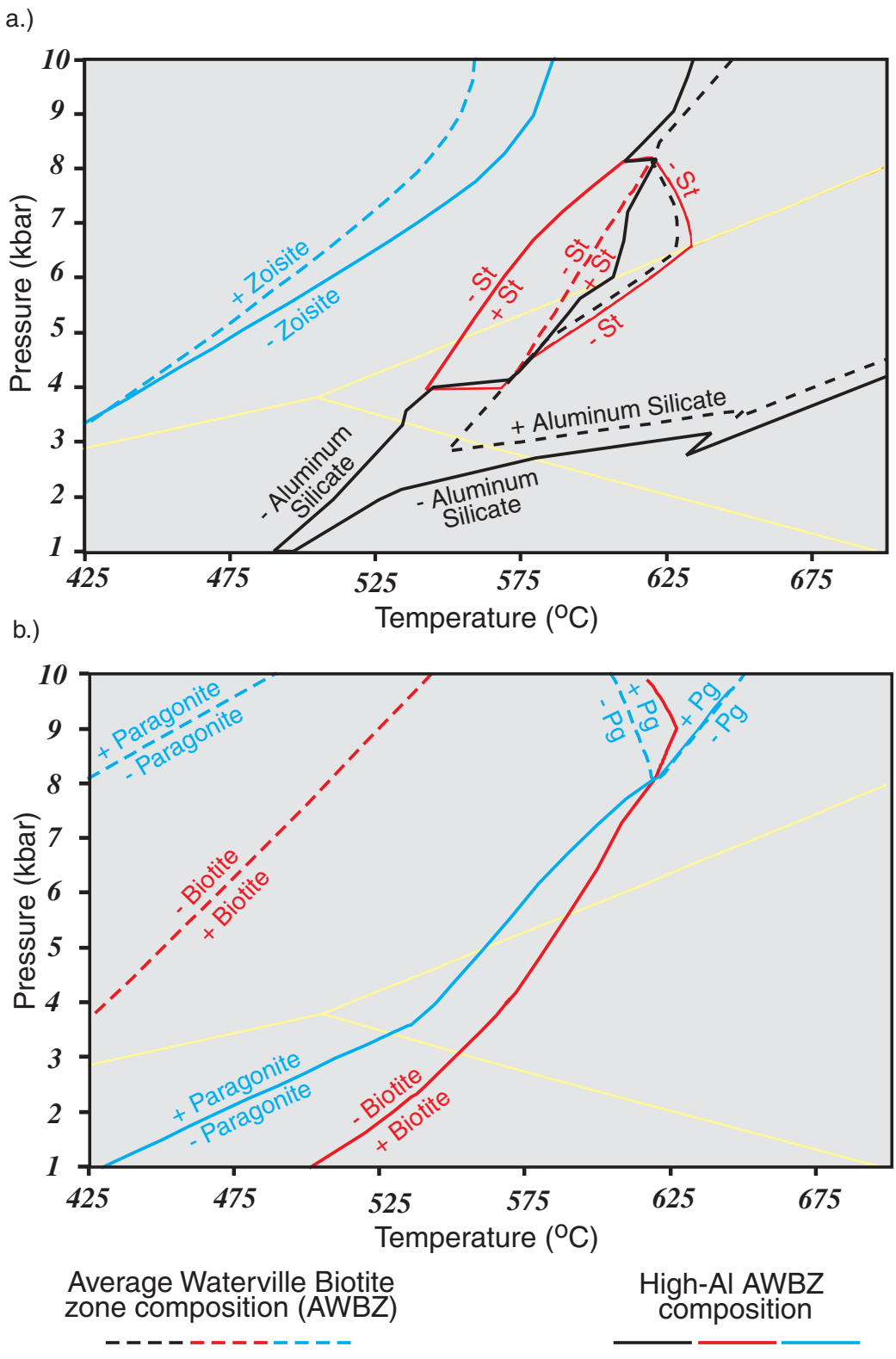

Figure 9. Comparison of staurolite, biotite, aluminum silicate, and zoisite zero mode isopleths for the AWBZ and High-Al AWBZ compositions in MnNCKFMASH.

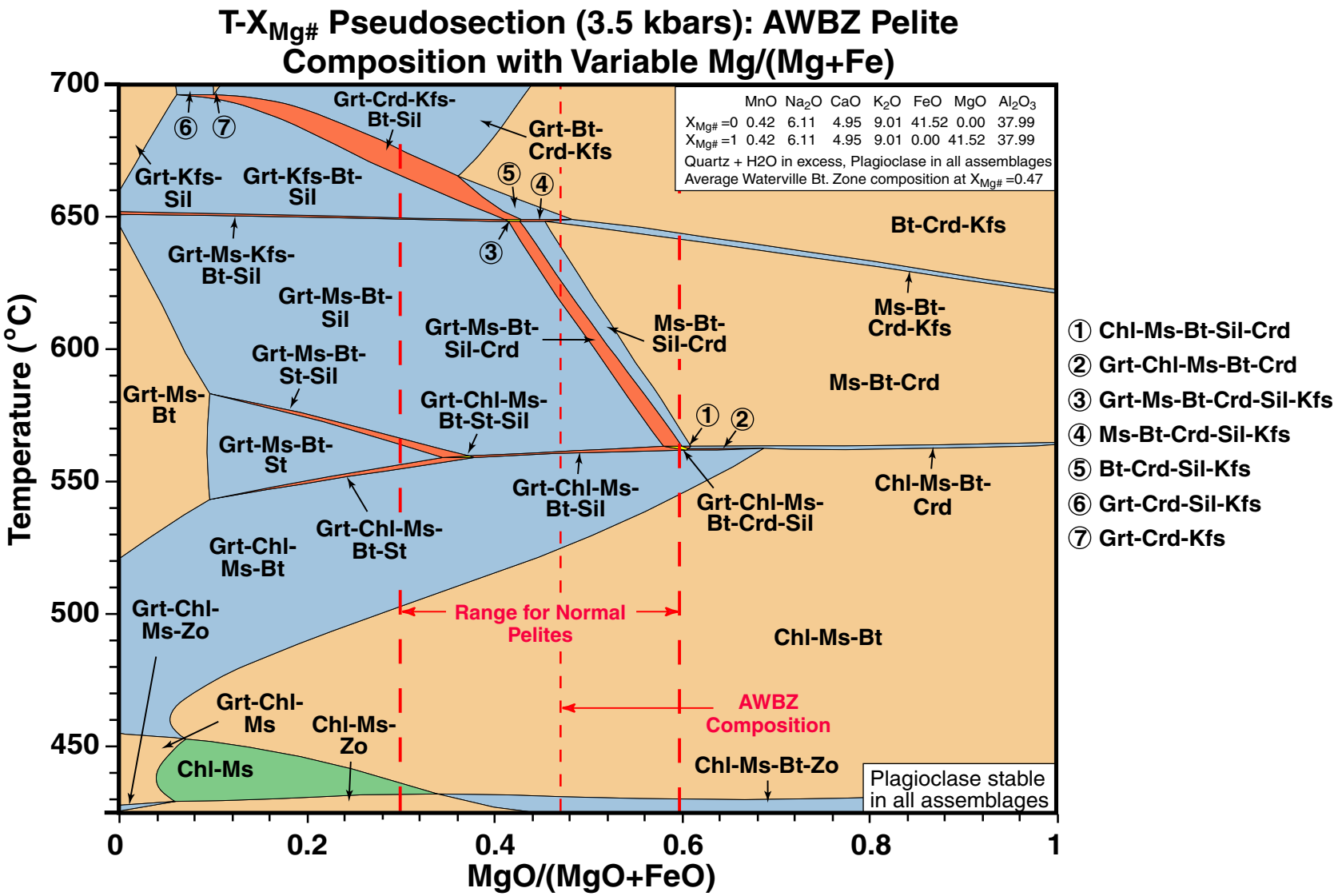

Figure 10. T-X$_{Mg\#}$ pseudosection for the AWBZ composition, from 0% MgO and 41.52% FeO at X$_{Mg\#}$=0 to 41.52% MgO and 0% FeO at X$_{Mg\#}$=1 (composition in mole %). The AWBZ Mg# and Mg# range for typical Waterville pelites are indicated.

at which muscovite breaks down to form potassium feldspar is dependent on $X_{Mg\#}$ when sillimanite is absent, controlled by the generalized reaction Bt + Ms = Crd + Kfs + H_2O. The breakdown temperature of muscovite to potassium feldspar is essentially independent of $X_{Mg\#}$ when sillimanite is present.

Biotite is stable over most of the pseudosection except at low $X_{Mg\#}$ at both low temperatures (< 455 °C) and high temperatures (> 660 °C). The stability of zoisite is mostly independent of $X_{Mg\#}$ and is restricted to low temperatures (< 435 °C).

T-$X_{Mg\#}$ pseudosection for the High-Al AWBZ (Fig.11). The High-Al AWBZ T-$X_{Mg\#}$ pseudosection has complicated topology at low $X_{Mg\#}$ relative to the T-$X_{Mg\#}$ AWBZ pseudosection due to the additional stability of chloritoid. Zoisite stability is essentially independent of $X_{Mg\#}$ and is stable at low temperatures. Paragonite stability extends to slightly lower temperatures with decreasing $X_{Mg\#}$ until sillimanite joins the assemblage, where it becomes almost independent of $X_{Mg\#}$ above about 0.47 $X_{Mg\#}$. Chlorite stability shows only moderate dependence on $X_{Mg\#}$, reacting out at lower temperatures with decreasing $X_{Mg\#}$ when sillimanite is absent. At very low $X_{Mg\#}$ (< 0.03) when biotite is absent (Grt-Ms-St-Pl-Qtz-H_2O), chlorite stability becomes strongly dependent on $X_{Mg\#}$, reacting out at lower temperatures with decreasing $X_{Mg\#}$. Where sillimanite is present, chlorite is stabilized to slightly higher temperatures with increasing $X_{Mg\#}$. Chloritoid is restricted to low $X_{Mg\#}$ (< 0.15) and is stable only over the interval 495-528 °C. Muscovite is stable with K-feldspar over a very restricted temperature interval. At $X_{Mg\#}$ < 0.6, muscovite reacts out at approximately 650-655 °C when sillimanite is in the assemblage. Where sillimanite is not stable at higher $X_{Mg\#}$, the upper temperature limit of muscovite stability decreases down to approximately 625 °C in the assemblage Ms-Bt-Pl-Crd-Kfs-Qtz-H_2O.

The low temperature stability limit for garnet increases from 480 °C at $X_{Mg\#}$ = 0 to approximately 560 °C at $X_{Mg\#}$ = 0.675, where cordierite joins the assemblage. Garnet is not stable at $X_{Mg\#}$ > 0.675 for this T-X pseudosection composition. With muscovite and cordierite in the assemblage, the upper temperature stability of garnet changes from 560°C at $X_{Mg\#}$ = 0.675 to 650 °C at $X_{Mg\#}$ = 0.425, where muscovite reacts out of the assemblage. With potassium feldspar in the assemblage, the slope of the Grt-out isopleth changes from negative to positive. With increasing temperature, garnet is restricted to lower $X_{Mg\#}$ up to about 675 °C, where it is stabilized to higher $X_{Mg\#}$ with increasing temperature. This change in slope of the garnet-out isopleth occurs in the assemblage Grt-Crd-Kfs-Bt-Pl-Sil-Qtz-H_2O. In this assemblage, sillimanite is reacting out with increasing temperature. In the assemblage Grt-Crd-Kfs-Bt-Pl-Qtz-H_2O, the garnet-out isopleth continues up temperature with a positive slope. Apparently, the change in slope of the garnet-out isopleth is related to sillimanite stability.

The low temperature biotite stability limit is nearly independent of $X_{Mg\#}$ when sillimanite is in the assemblage. At lower $X_{Mg\#}$, in the absence of sillimanite, biotite is stabilized to slightly lower temperatures with decreasing $X_{Mg\#}$ until extremely low $X_{Mg\#}$ (< 0.03), where biotite is unstable except in the interval 628-662 °C. The lowest temperature stability of cordierite is at about 550 °C with $X_{Mg\#}$ = 1. Cordierite stability changes only slightly with decreasing $X_{Mg\#}$ until garnet joins the assemblage, where the lower temperature limit shifts to much higher temperatures with decreasing $X_{Mg\#}$. Cordierite is stabilized to extremely low $X_{Mg\#}$ (0.05) at 700 °C. Staurolite is restricted to the temperature interval 525-583 °C at the high Fe end of the pseudosection. Staurolite is not stable at $X_{Mg\#}$ > 0.425. Most Waterville pelite bulk rock compositions have $X_{Mg\#}$ = 0.33-0.56, indicating the lowest $X_{Mg\#}$ rocks could contain staurolite at 3.5 kbars if they had an extremely high Al content.

Sample 980A (Staurolite-Andalusite Zone)

A P-T pseudosection for a sample from the staurolite-andalusite zone (980A) is shown in Figure 12. Sample 980A contains a Grt-Ms-Bt-St-And-Pl-Qtz bearing assemblage (Ferry, 1980). This sample was chosen because it contains both staurolite and andalusite and is one of the samples for which thermobarometry was performed using mineral compositions reported in Ferry (1980). Overall, the composition of 980A is representative of pelitic samples from the staurolite-andalusite zone, although it has slightly higher MnO content, higher CaO content, and lower MgO content than the average staurolite-andalusite zone composition. The 980A SiO_2-free molar composition has a lower Al_2O_3 content than the AWBZ, and this is reflected by decreased aluminum silicate, staurolite, and paragonite stability. Kyanite is not predicted to be stable in the P-T window, and staurolite is predominantly restricted to the sillimanite field. Paragonite does not appear as a stable phase in the P-T window. With the higher MnO and CaO content, garnet is stabilized to below the aluminum silicate triple point and to pressures < 1 kilobar. In addition, garnet has a larger stability than the AWBZ at high temperatures and low pressures when sillimanite is not in the assemblage.

Comparison to Waterville Formation

Predicted mineral assemblages are compared to those observed in the Waterville Fm. to determine the ability

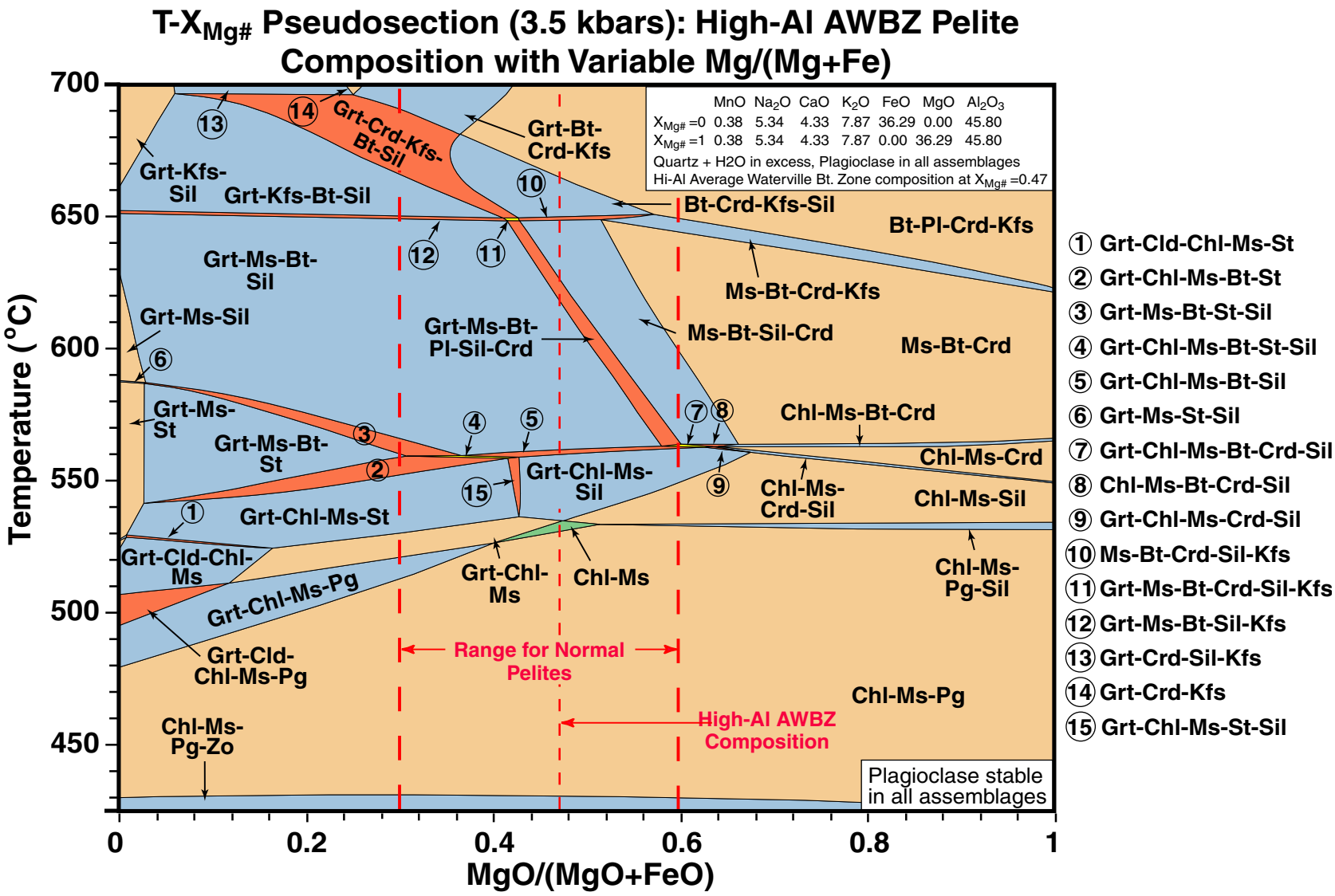

Figure 11. T-X$_{Mg\#}$ pseudosection for the High-Al AWBZ composition, from 0% MgO and 36.29% FeO at X$_{Mg\#}$=0 to 36.29% MgO and 0% FeO at X$_{Mg\#}$=1 (composition in mole%). The High-Al AWBZ Mg# and Mg# range for typical Waterville pelites are indicated.

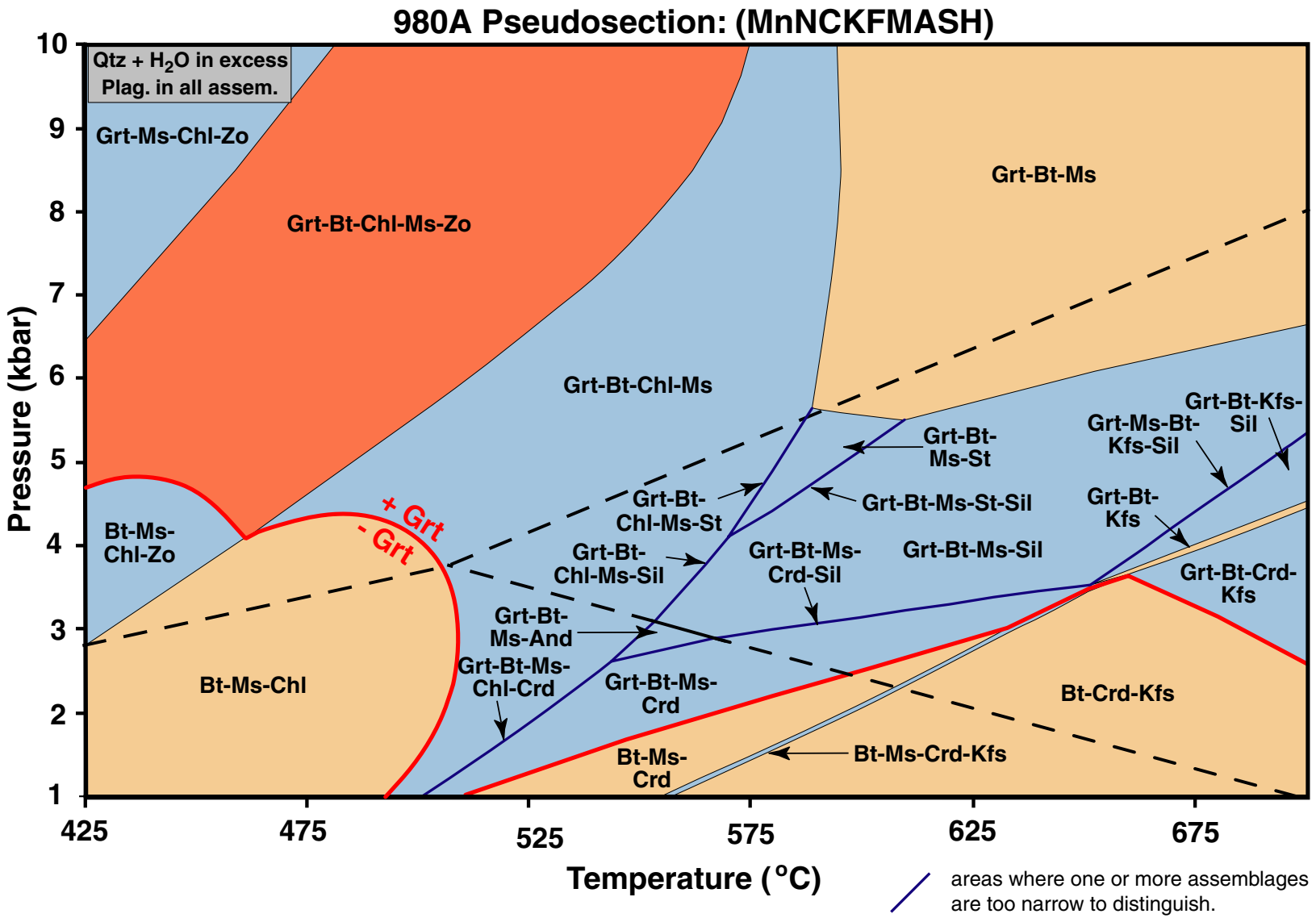

Figure 12. MnNCKFMASH P-T pseudosection for a Waterville Fm. sample (980A) from the staurolite-andalusite zone.

of MnNCKFMASH pseudosections to realistically predict stable assemblages. Figures 13 and 14 show P-T pseudosections (AWBZ and 980A, respectively) with assemblage fields colored only in the pressure interval 2.7 to 4.7 kbars. This interval was chosen to represent the approximate pressure of metamorphism (derived from GASP-GaBi thermobarometry, discussed below). The observed (Osberg, 1971; Ferry, 1982) and MnNCKFMASH-predicted sequence of assemblages for the different zones are compared in Tables 2a and 2b. The main differences are the predicted presence of zoisite in the biotite zone, predicted absence of staurolite below 4.1 kbars, and the predicted restriction of andalusite stability to < 3 kbars in the pseudosections. Ferry (1982) did not note zoisite/clinozoisite in the biotite zone, whereas the pseudosections predict a rather small stability field of zoisite. Nonetheless, Ms-Pl-Bt-Chl-Qtz-H_2O is the predicted assemblage for most of the biotite zone, matching that observed by Ferry. The assemblage Ms-Pl-Bt-Chl-Grt-Qtz-H_2O is the predominant predicted assemblage for the garnet zone, which also matches that observed by Ferry. Above the garnet zone, predicted and observed assemblages do not match as well. Staurolite is predicted above 4.1 kbars for 980A and 4.5 kbars for AWBZ, while andalusite is predicted below 3 kbars. Therefore, the observed paragenesis St + And is not predicted for the pseudosection compositions considered here. Instead, the pseudosections predict the staurolite zone assemblage of Ms-Pl-Bt-Grt-St-Qtz-H_2O ± Chl at pressures > 4.1 kbars, matching that observed by Ferry with the exception of andalusite. This assemblage is only stable for about 10 degrees at 4.7 kbars below sillimanite stability. Below 3.1 kbars, the pseudosections predict the hypothetical andalusite (± Crd) zone assemblages Ms-Pl-Bt-Grt-And-Qtz-H_2O ± Crd ± Chl. Ferry (1982) noted cordierite is locally found in the staurolite-andalusite zone, and therefore the predicted assemblage below 3.1 kbars matches the observed assemblage with the exception of staurolite. Pattison et al. (1999) conclude that in south-central Maine (and several other localities) the association Ms-Crd-St-Bt is unstable for typical pelite compositions. They conclude that the association is unlikely to become stable by the addition of small amounts of Mn or Zn to the system, and that Crd + St likely occurs in this association due to poly-metamorphism. The calculated pseudosection (calculated without consideration of Zn) is compatible with their interpretation. Between 3 and 4.1 kbars, neither staurolite nor andalusite is predicted, and the garnet zone is followed directly by the sillimanite zone assemblage Ms-Pl-Bt-Grt-Sil-Qtz-H_2O. Above the sillimanite-in isograd, positive slopes of the Grt-, Crd-, and Sil —out isopleths lead to the assemblages Ms-Pl-Bt-Qtz-H_2O ± Grt ± Sil ± Crd at low pressures and high temperatures, matching the assemblages observed by Ferry with the exception of staurolite.

Overall, the sequence of assemblages predicted by the pseudosections is in good agreement with those observed by Ferry over the pressure interval 2.7-4.7 kbars. The only major exception to this is the reported co-existence of staurolite and andalusite, which is discussed below.

Correlation with Thermobarometry

The standard technique for determining equilibration conditions for a pelitic rock is conventional thermobarometry, typically involving garnet-rim and matrix phase compositions. We have calculated pressures and temperatures for a subset of samples from the Waterville Fm. to compare garnet-rim thermobarometry results with the AWBZ pseudosection. The uncertainties associated with thermobarometry are substantial, and the comparison is therefore not meant to be a test of the pseudosection method. However, the comparison does illustrate the type of correlation that is to be expected between thermobarometry from a suite of samples with varying composition and a pseudosection calculated for an average of this suite of rocks.

P-T conditions were estimated by simultaneous calculation of the garnet-biotite thermometer (GaBi) and garnet-aluminum silicate-quartz-plagioclase barometer (GASP) for 18 Waterville Fm. samples. Thermo-barometry methods are outlined in Appendix 2. Mineral compositions are taken from Ferry (1980). The same thermodynamic data (Holland and Powell, 1998) and activity models (Appendices 1 and 2) used for pseudosection calculations were utilized for P-T calculations. The biotite activity model was modified to account for Ti.

Eighteen samples from the staurolite-andalusite, staurolite-cordierite, and sillimanite zones were selected (Fig. 1). Samples in the staurolite-cordierite zone contain andalusite. P-T results, shown in Table 3 and Figure 15, yield a mean pressure of 3.7 ± 0.5 kbars (1 std. dev.). This pressure is in very good agreement with that calculated by Ferry (1980). Five of the nine samples containing sillimanite plot within the sillimanite field, one plots on the sillimanite-andalusite boundary, one plots in the kyanite field, and two plot within the andalusite field. Two of the sillimanite-bearing samples actually plot in a pseudosection field containing sillimanite, and one plots in a pseudosection field containing andalusite. The other sillimanite-bearing samples all plot in aluminum-silicate-absent pseudosection fields. For the nine andalusite-bearing samples, five plot in the andalusite

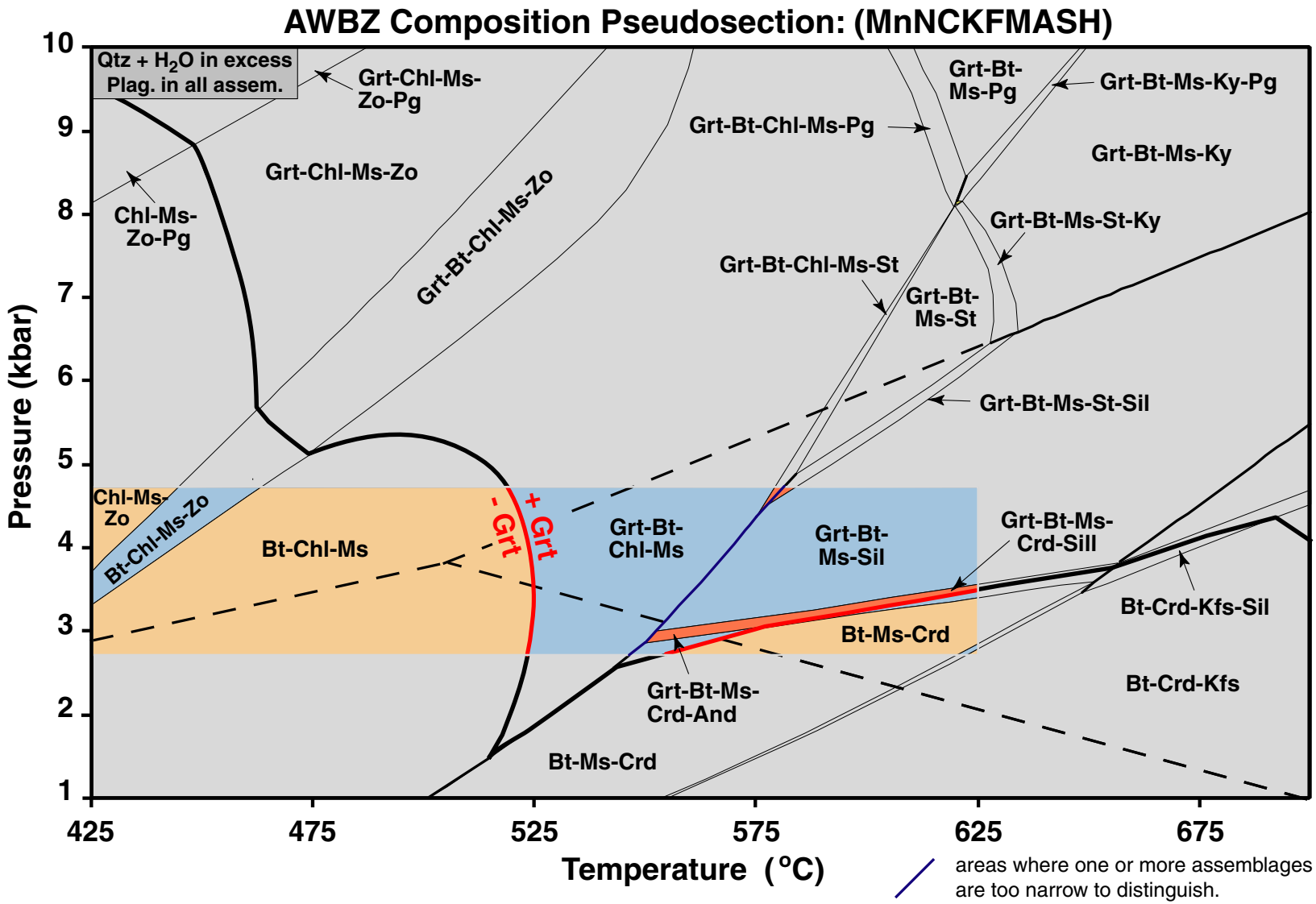

Figure 13. MnNCKFMASH pseudosection for the AWBZ composition, highlighting the sequence of predicted assemblages at pressures experienced by Waterville Fm. samples.

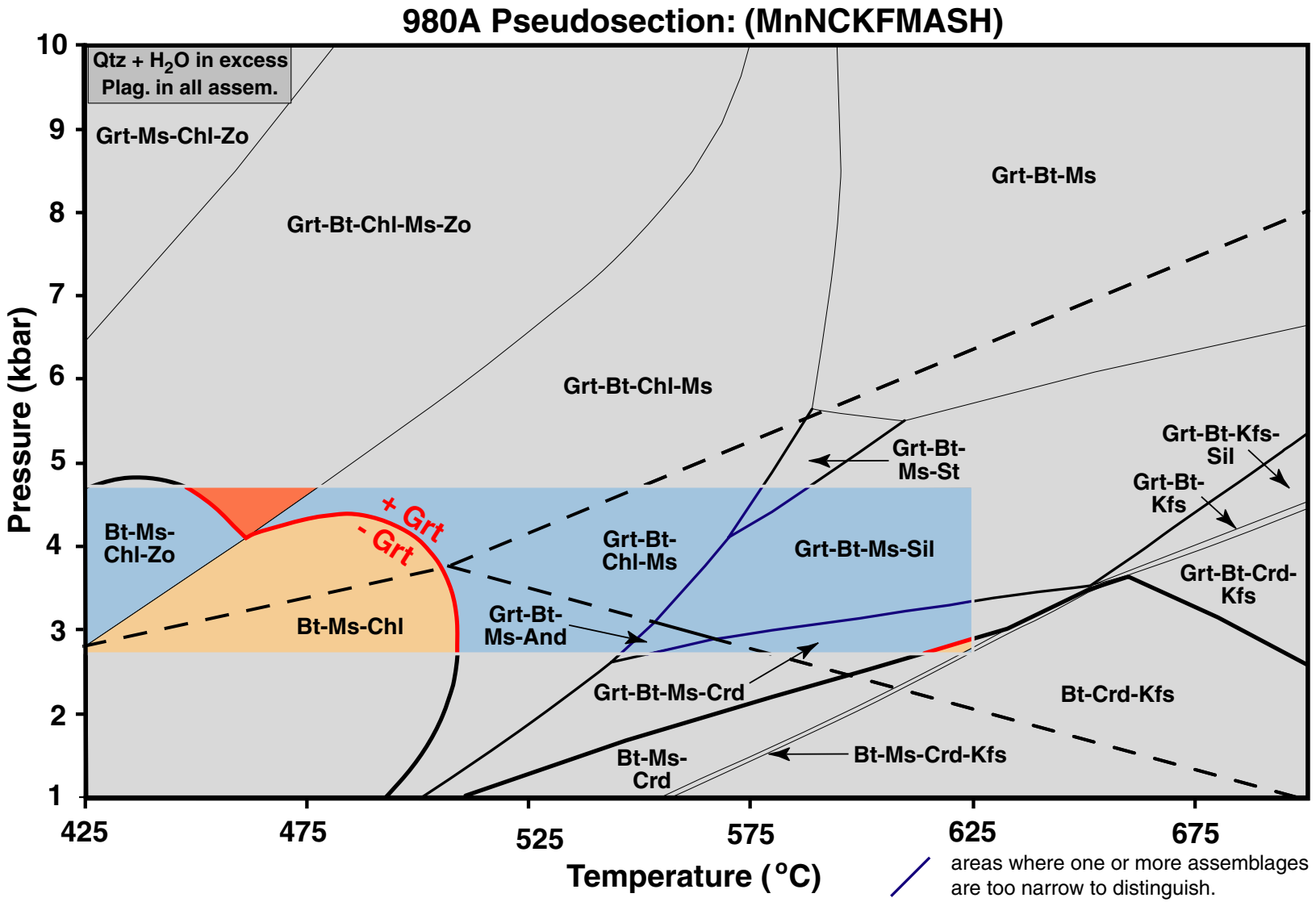

Figure 14. MnNCKFMASH pseudosection for the 980A composition, highlighting the sequence of predicted assemblages at pressures experienced by Waterville Fm. samples.

Table 2. Comparison of predicted and observed Waterville Fm. assemblages for (2a) AWBZ pseudosection, and (2b) 980A pseudosection. Predicted assemblages are separated into high to low pressure (listed top to bottom) assemblages as needed.

2a. Comparison with AWBZ parageneses

Met. Zone	Observed Paragenesis[1]	Predicted Paragenesis[1, 2]
Biotite	Bt ± Chl	(2.7-4.7 kbars) Bt + Chl ± Zo
Garnet	Bt ± Chl ± Grt	(2.7-4.7 kbars) Grt + Bt + Chl
Staurolite-Andalusite	Bt ± Chl ± Grt ± St ± And	Staurolite + Andalusite bearing: not predicted Staurolite bearing: (3.7-4.7 kbars) Grt + Chl + Bt + St Andalusite bearing: (2.7-3.7 kbars) Grt + Bt + And ± Chl
Staurolite-Cordierite	Bt ± Chl ± Grt ± St ± And ± Crd	Staurolite + Cordierite bearing: not predicted Cordierite bearing: (2.7-3.7 kbars) Bt + Crd ± Grt ± And ± Chl
Sillimanite	Bt ± Grt ± St ± Sil ± Crd ± Kfs	(3.7-4.7 kbars) Grt + Bt + Sil ± Chl ± St (3.7 kbars) Grt + Bt + Sil (2.7-3.7 kbars) Bt + Crd ± Sil (2.7-3.7 kbars) Grt + Bt ± Crd ± Sil

[1] Each paragenesis contains muscovite, plagioclase, and quartz.
[2] Assemblages are specified as occurring between 3.7 & 4.7 kbars, at 3.7 kbars, or between 2.7 & 3.7 kbars.

2b. Comparison with 980A parageneses

Met. Zone	Observed Paragenesis[1]	Predicted Paragenesis[1, 2]
Biotite	Bt ± Chl	(2.7-4.7 kbars) Bt + Chl ± Zo
Garnet	Bt ± Chl ± Grt	(2.7-4.7 kbars) Grt + Bt + Chl
Staurolite-Andalusite	Bt ± Chl ± Grt ± St ± And	Staurolite + Andalusite bearing: not predicted Staurolite bearing: (3.7-4.7 kbars) Grt + Bt + St ± Chl Andalusite bearing: (2.7-3.7 kbars) Grt + Bt + And ± Chl
Staurolite-Cordierite	Bt ± Chl ± Grt ± St ± And ± Crd	Staurolite + Cordierite bearing: not predicted Cordierite bearing: (2.7-3.7 kbars) Grt + Bt + Crd ± And
Sillimanite	Bt ± Grt ± St ± Sil ± Crd ± Kfs	(3.7-4.7 kbars) Grt + Bt + Sil ± Chl ± St (3.7 kbars) Grt + Bt + Sil ± Chl (2.7-3.7 kbars) Grt + Bt ± Crd ± Sil ± Chl

[1] Each paragenesis contains muscovite, plagioclase, and quartz.
[2] Assemblages are specified as occurring between 3.7 & 4.7 kbars, at 3.7 kbars, or between 2.7 & 3.7 kbars.

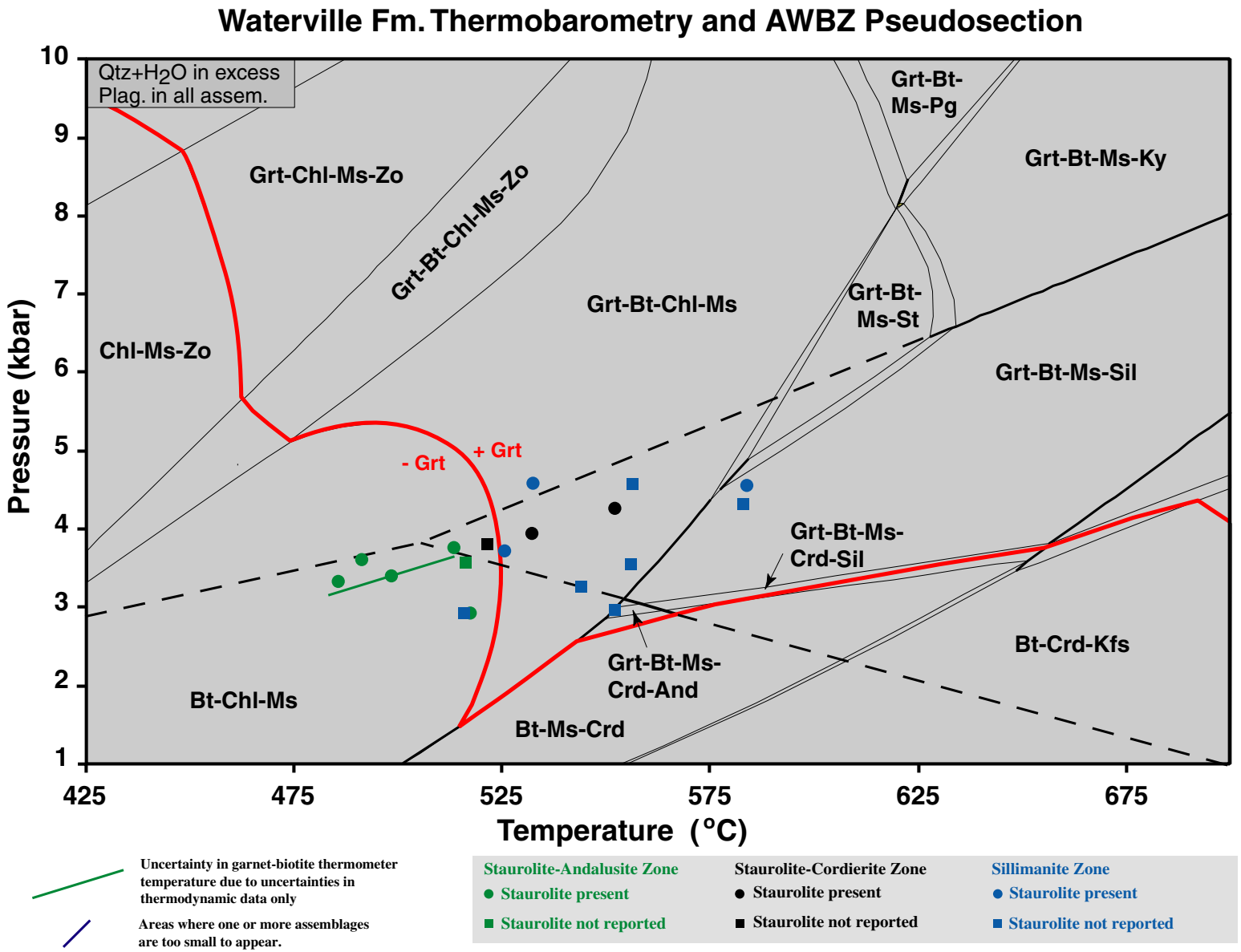

Figure 15. MnNCKFMASH pseudosection for the AWBZ composition with garnet thermobarometry results indicated.

Table 3. Garnet-biotite and garnet-aluminum silicate-quartz-plagioclase thermobarometry.

Sample	Met. Zone	Staurolite	Temperature (°C)	Pressure (kbar)
56A-1	St-And	No	516	3.6
246A	St-And	Yes	514	3.8
980A	St-And	Yes	486	3.3
1006A	St-And	Yes	499	3.4
1010A	St-And	Yes	518	2.9
953A	St-And	Yes	491	3.6
917A	St-Crd	No	521	3.8
928B	St-Crd	Yes	552	4.3
1001A	St-Crd	Yes	532	3.9
663A	Sil	Yes	583	4.6
666A	Sil	Yes	525	3.7
1104-1	Sil	Yes	532	4.6
675-4	Sil	No	543	3.2
675-5	Sil	No	582	4.3
905A	Sil	No	556	4.6
388A	Sil	No	516	2.9
674A	Sil	No	556	3.5
9.69B	Sil	No	551	3.0

field and four plot in the sillimanite field. All three of the samples from the staurolite-cordierite zone plot in the sillimanite field. The consistency between thermobarometry and the pseudosection is much worse for the andalusite bearing samples; all of the andalusite bearing samples plot in a pseudosection field lacking andalusite. In addition, at least 10 of the 18 samples contain staurolite, but do not plot in a staurolite bearing field.

Although all 18 samples contain garnet, 7 samples plot in garnet absent fields. The position of the garnet-in isopleth on the pseudosection is strongly dependent on bulk rock Mn content, and to a lesser extent Ca and Fe content. Sample 980A has slightly higher MnO and FeO, and considerably higher CaO content than the AWBZ. The 980A pseudosection (Fig. 12) shows the garnet-in isopleth to be stable at lower temperatures than the AWBZ pseudosection, compatible with its higher Mn, Ca, and Fe content. However, thermobarometry yields a P & T of 3.3 kbars, 487 °C for sample 980A, which is below the 980A garnet-in isopleth.

Overall, correlation between garnet rim thermobarometry and predicted assemblage stability is quite poor. Titanium is commonly present in appreciable amounts in biotite, which may have a significant effect on garnet-biotite thermometry. White and others (2000) extended the KFMASH biotite activity model used here to include Ti and Fe^{3+} iron end members. Use of this activity model increases calculated temperatures and pressures an average of 31 °C and 0.5 kbars, respectively. The calculated pressure and temperature of 980A would increase to 3.7 kbars, 509 °C, which places it within the Grt-Chl-Ms-Bt-Pl stability field. Although this biotite activity model increases the calculated temperature enough to plot in a garnet bearing assemblage, it does not place it in a staurolite- or andalusite-bearing assemblage.

We are uncertain if the lack of correlation between thermobarometry and pseudosection assemblage fields is due to uncertainty in thermobarometric results, use of improper bulk rock compositions for pseudosection construction, inadequate thermodynamic data, or disequilibrium crystallization in the rock. However, it is clear that in general, utilization of pseudosections and thermobarometry for deciphering P-T histories of metamorphism will require careful consideration of the thermobarometric accuracy and consideration of the bulk composition used for pseudosection construction. For example, if there is a significant amount of chemical zoning in minerals from the suite of Waterville samples, it is likely that the bulk-rock composition determined from X-ray fluorescence analysis is not the effective bulk rock composition experienced by the reacting suite of minerals and fluid at the peak of metamorphism (e.g., Stuwe, 1997). This does not mean that bulk compositions determined by X-ray fluorescence analysis are not appropriate for some purposes of pseudosection modeling. Vance and Mahar (1998), Tinkham and Stowell

(2000), and Stowell et al. (2001) have used bulk compositions determined by X-ray fluorescence to successfully model the early stages of garnet growth, before garnet sequestered significant amounts of Mn, Mg, Fe, and Ca, thus modifying the effective bulk composition of the rock.

Discussion

One of the arguments against using a complex chemical system for modeling natural rocks is the effect of uncertainty in thermodynamic data and mixing relationships in complex solid solutions on predicted mineral stability. KFMASH has long been considered the system of choice for quantitative modeling of pelites, and as discussed above, has been quite successful at predicting the sequential occurrence of Fe-Mg solid solution phases over metamorphic field gradients. The major problems with utilizing the KFMASH system for pseudosection analysis are (1) inability to predict realistic garnet stability at low temperatures and pressures, (2) strong dependence of predicted phase stability on the method of projecting a real composition into KFMASH space, and (3) inability to model the effect of non-KFMASH phases on KFMASH phase stability, such as the effect of paragonite on aluminum-silicate stability discussed above. Addition of MnO, CaO, and Na_2O allows modeling of garnet composition and the common pelite minerals plagioclase, zoisite/clinozoisite, and less common minerals such as paragonite and margarite. Simultaneous modeling of garnet and plagioclase is important because anorthite and grossular are commonly used to constrain metamorphic pressures. In addition, use of MnNCKFMASH does not require projection (in terms of major chemical components) of a rock composition into the system as required for KFMASH. MnNCKFMASH is the minimum system that should be used for quantitative pseudosection prediction of the P-T stability and compositions of pelitic minerals. This is particularly true for modeling garnet composition. Vance and Holland (1993) and Vance and Mahar (1998) were aware of this, and, to our knowledge, were the first to quantitatively apply MnNCKFMASH pseudosections to derive P-T paths. However, we do not mean to imply that pelite phase relations cannot be investigated in KFMASH. Spear (1999) has shown how Mn in garnet (and other phases) can effectively be dealt with in a quantitative manner to investigate Fe-Mg partitioning relations in KFMASH. So, for some purposes, KFMASH is a suitable system for modeling pelites.

The MnNCKFMASH model system is quite successful in predicting the sequence of assemblages observed in the Waterville Formation. A major exception is failure to predict the paragenesis St + And and St + And + Crd. Pattison et al. (1999) make a strong argument for metastable persistence of staurolite (polymetamorphism) in the cordierite stability field, and suggest that the paragenesis Ms + Bt + St + Crd ± And is unstable. If their interpretation is correct, the pseudosections presented here correctly predict this paragenesis is not stable for Waterville Fm. compositions even though it does occur in the Waterville Fm. However, the inability of pseudosections presented here to predict St + And remains problematic. Possible reasons for this discrepancy include inaccurate thermodynamic data and activity models, metastable persistence of staurolite and/or andalusite, polymetamorphism, and the effect of non-system components on staurolite stability, in particular ZnO (e.g., Proyer and Dachs, 2000). Pattison et al. (1999) address the ability of Zn to increase the stability of Ms + Bt + Crd + St assemblages, and conclude that the small amounts of Zn in Waterville Fm. staurolites is unlikely to substantially effect staurolite stability. Therefore, we suggest that inability of the pseudosections to predict St + And is not due to omission of ZnO in the models. Pattison et al. (1999) presented possible polymetamorphic P-T paths, including isothermal decompression and metastable persistence of staurolite to lower pressures, and two distinct heating events, the first at a higher pressure in the staurolite stability field, and the second at lower pressure in the cordierite stability field. The pseudosections presented here, with staurolite only stable at pressures higher than andalusite and cordierite stability, is consistent with a polymetamorphic P-T path. However, the pseudosections suggest that an isothermal decompression path is unlikely, because such a path would require the staurolite bearing rocks to pass through the sillimanite stability field during decompression, indicating andalusite would form after sillimanite. This is unlikely because sillimanite and andalusite are not found associated with one another, the sillimanite-andalusite boundary is very sharply defined, and this scenario would require widespread metastable persistence of staurolite, but not sillimanite. A polymetamorphic path that led to heating and staurolite growth at about 5 kbars, cooling and decompression to about 3 kbars, followed by reheating to produce andalusite and cordierite growth, would be compatible with the pseudosections. However, the andalusite stability fields predicted by the pseudosections for the AWBZ and sample 980A (St + And bearing rock) are very small, indicating that the reaction kinetics and mechanisms leading to the persistence of staurolite and formation of later andalusite in a very small P-T window would have to be very similar for the large number of samples containing St + And (Fig. 1). Although this is not impossible, we feel it is more likely that the andalusite stability field is larger than that predicted by the pseudosections.

The Holland and Powell (1998) data set aluminum-silicate triple point is at 3.8 kbars, 505 °C. This is at a lower pressure and temperature than the Holland and Powell (1990) data set (4.5 kbars, 553 °C), the Pattison et al. (in press) data set (4.6 kbars, 545 °C), and the Pattison (1992) triple point (4.5 kbars, 550 °C). Use of these data sets with the triple point at higher pressures and temperatures would likely lead to an andalusite field extended to slightly higher temperatures and pressures, reducing the St + And discrepancy.

We would like to use the results from this study to further address any possible inadequacies of the Holland and Powell (1998) data set to realistically model metapelites with MnNCKFMASH pseudosections. However, the geologic complexity, including possible polymetamorphism experienced by the Waterville Fm. samples, preclude a more detailed evaluation than given above. The results presented here clearly show that MnNCKFMASH pseudosections are useful for modeling metapelite mineral assemblage stability and mineral stability dependence on bulk composition. Additional studies of this type may allow assessment of currently available thermodynamic data for modeling in chemical systems suitable for natural rocks.

Acknowledgments

We thank John M. Ferry for providing bulk rock XRF analyses from the Waterville Fm., Maine, an anonymous reviewer, and D.R.M. Pattison for a detailed review that led to improvement of the manuscript. We acknowledge partial support from the Graduate School and Department of Geological Sciences, University of Alabama, the Geological Society of America, Sigma XI, and National Science Foundation Grants EAR-9805021 (to D.L. Harry and H.H. Stowell) and EAR-9628232 (to N.L. Green, H.H. Stowell, and others).

References cited

Atherton, M.P., and Brotherton, M.S. (1982) Major element composition of the pelites of the Scottish Dalradian. Geological Journal, 17, 185-221.

Berman, R.G. (1988) Internally-consistent thermodynamic data for minerals in the system Na_2O-K_2O-CaO-MgO-FeO-Fe_2O_3-Al_2O_3-SiO_2-TiO_2-H_2O-CO_2. Journal of Petrology, 29, 445-522.

Droop, G.T.R., and Harte, B. (1995) The effect of Mn on the phase relations of medium-grade pelites: Constraints from natural assemblages on petrogenetic grid topology. Journal of Petrology, 36, 1549-1578.

Ferry, J.M. (1980) A comparative study of geothermometers and geobarometers in pelitic schists from South-central Maine. American Mineralogist, 65, 720-732.

Ferry, J.M. (1982) A comparative geochemical study of pelitic schists and metamorphosed carbonate rocks from south-central Maine, USA. Contributions to Mineralogy and Petrology, 80, 59-72.

Ferry, J.M. (1984) A biotite isograd in south-central Maine, U.S.A.; mineral reactions, fluid transfer, and heat transfer. Journal of Petrology, 25, 871-893.

Gottschalk, M. (1997) Internally consistent thermodynamic data for rock-forming minerals in the system SiO_2-TiO_2-Al_2O_3-CaO-MgO-FeO-K_2O-Na_2O-H_2O-CO_2. European Journal of Mineralogy, 9, 175-223.

Hensen, B. J. (1971) Theoretical phase relations involving cordierite and garnet in the system MgO-FeO-Al_2O_3-SiO_2. Contributions to Mineralogy and Petrology, 33, 191-214.

Holland, T., Baker, J., and Powell, R. (1998) Mixing properties and activity-composition and relationships of chlorites in the system MgO-FeO-Al_2O_3-SiO_2-H_2O. European Journal of Mineralogy, 10, 395-406.

Holland, T., and Powell, R. (1992) Plagioclase feldspars; activity-composition relations based upon Darken s quadratic formalism and Landau theory. American Mineralogist, 77, 53-61.

Holland, T.J.B., and Powell, R. (1985) An internally consistent thermodynamic dataset with uncertainties and correlations; 2, Data and results. Journal of Metamorphic Geology, 3, 343-370.

Holland, T.J.B., and Powell, R. (1990) An enlarged and updated internally consistent thermodynamic dataset with uncertainties and correlations; the system K_2O-Na_2O-CaO-MgO-MnO-FeO-Fe_2O_3-Al_2O_3-TiO_2-SiO_2-C-H_2-O_2. Journal of Metamorphic Geology, 8, 89-124.

Holland, T.J.B., and Powell, R. (1998) An internally consistent thermodynamic data set for phases of petrological interest. Journal of Metamorphic Geology, 16, 309-343.

Kretz, R. (1983) Symbols for rock-forming minerals. American Mineralogist, 68, 277-279.

Mahar, E.M., Baker, J.M., Powell, R., Holland, T.J.B., and Howell, N. (1997) The effect of Mn on mineral stability in metapelites. Journal of Metamorphic Geology, 15, 223-238.

Menard, T., and Spear, F.S. (1993) Metamorphism of calcic pelitic schists, Strafford Dome, Vermont; compositional zoning and reaction history. Journal of Petrology, 34, 977-1005.

Osberg, P.H. (1971) An equilibrium model for Buchan-type metamorphic rocks, south-central, Maine.

American Mineralogist, 56, 570-585.

Pattison, D.R.M. (1992) Stability of andalusite and sillimanite and the Al_2SiO_5 triple point; constraints from the Ballachulish aureole, Scotland. Journal of Geology, 100, 423-446.

Pattison, D.R.M. (2001) Instability of Al_2SiO_5 triple-point assemblages in muscovite + biotite + quartz-bearing metapelites, with implications. American Mineralogist, 86, 1414-1422.

Pattison, D.R.M., and Tracy, R.J. (1991) Phase equilibria and thermobarometry of metapelites. In: D.M. Kerrick, Ed., Contact metamorphism. Mineralogical Society of America Reviews in Mineralogy, 26, 105-206.

Pattison, D.R.M., Spear, F.S., DeBuhr, C.L., Cheney, J.T., and Guidotti, C.V. (2002) Thermodynamic modelling of the reaction Muscovite+Cordierite-> Al_2SiO_5 +Biotite+Quartz+H_2O: constraints from natural assemblages and implications for the metapelitic petrogenetic grid. Journal of Metamorphic Geology, 20, in press.

Pattison, D.R.M., Spear, F.S., and Cheney, J.T. (1999) Polymetamorphic origin of muscovite + cordierite + staurolite + biotite assemblages; implications for the metapelitic petrogenetic grid and for P-T paths. Journal of Metamorphic Geology, 17, 685-703.

Powell, R., and Holland, T. (1993) On the formulation of simple mixing models for complex phases. American Mineralogist, 78, 1174-1180.

Powell, R., and Holland, T. (1999) Relating formulations of the thermodynamics of mineral solid solutions; activity modeling of pyroxenes, amphiboles, and micas. American Mineralogist, 84, 1-14.

Powell, R., Holland, T., and Worley, B. (1998) Calculating phase diagrams involving solid solutions via non-linear equations, with examples using THERMOCALC. Journal of Metamorphic Geology, 16, 577-588.

Powell, R., and Holland, T.J.B. (1988) An internally consistent dataset with uncertainties and correlations; 3, Applications to geobarometry, worked examples and a computer program. Journal of Metamorphic Geology, 6, 173-204.

Proyer, A., and Dachs, E. (2000) Contrasting parageneses in mica schists of the Hohe Tauren, caused by manganese and zinc. Mineralogy and Petrology, 69, 197-212.

Spear, F.S. (1988) Thermodynamic projection and extrapolation of high-variance mineral assemblages. Contributions to Mineralogy and Petrology, 98, 346-351.

Spear, F.S. (1993) Metamorphic phase equilibria and pressure-temperature-time paths. 799 p. Mineralogical Society of America, Washington D.C.

Spear, F.S. (1999) Real-time AFM diagrams on your Macintosh. Geological Materials Research, 1, 1-18.

Spear, F.S., and Cheney, J.T. (1989) A petrogenetic grid for pelitic schists in the system SiO_2-Al_2O_3-FeO-MgO-K_2O-H_2O. Contributions to Mineralogy and Petrology, 101, 149-164.

Spear, F.S., Pyle, J.M., and Storm, L.C. (2001) Thermodynamic modeling of mineral reactions: An introduction to Program Gibbs. Northeast Section Meeting of the Geological Society of America Short Course 504, March 12, 2001, Burlington, Vermont.

Stowell, H.H., Menard, T., and Ridgway, C.K. (1996) Ca-metasomatism and chemical zonation of garnet in contact-metamorphic aureoles, Juneau Gold Belt, Southeastern Alaska. The Canadian Mineralogist, 34, 1195-1209.

Stowell, H.H., Taylor, D.L., Tinkham, D.K., Goldberg, S.A., and Ouderkirk, K.A. (2001) Contact metamorphic P-T-t paths from Sm-Nd garnet ages, phase equilibria modeling, and thermobarometry. Journal of Metamorphic Geology, 19, 645-660.

Stuwe, K. (1997) Effective bulk composition changes due to cooling: a model predicting complexities in retrograde reaction textures. Contributions to Mineralogy and Petrology, 129, 43-52.

Symmes, G.H., and Ferry, J.M. (1991) Evidence from mineral assemblages for infiltration of pelitic schists by aqueous fluids during metamorphism. Contributions to Mineralogy and Petrology, 108, 419-438.

Symmes, G.H., and Ferry, J.M. (1992) The effect of whole-rock MnO content on the stability of garnet in pelitic schists during metamorphism. Journal of Metamorphic Geology, 10, 221-237.

Thompson, A.B. (1976) Mineral reactions in pelitic rocks: I. Prediction of P-T-X(Fe-Mg) phase relations. II. Calculation of some P-T-X(Fe-Mg) phase relations. Americal Journal of Science, 276, 401-424, 425-454.

Tinkham, D.K., and Stowell, H.H. (2000) Lack of evidence for loading during garnet growth: Southern Nason terrane, Cascades Crystalline Core, Washington. Geological Society of America, Cordilleran Section, 2000 Annual Meeting, 32, p. A-71.

Trzcienski, W. E., Jr. (1977) Garnet zoning - product of continuous reaction. Canadian Mineralogist, 15, 250-256.

Vance, D., and Holland, T. (1993) A detailed isotopic and petrological study of a single garnet from the Gassetts Schist, Vermont. Contributions to Mineralogy and Petrology, 114, 101-118.

Vance, D., and Mahar, E. (1998) Pressure-temperature paths from P-T pseudosections and zoned garnets; potential, limitations and examples from the Zanskar

Himalaya, NW India. Contributions to Mineralogy and Petrology, 132, 225-245.

White, R.W., Powell, R., Holland, T.J.B., and Worley, B.A. (2000) The effect of TiO_2 and Fe_2O_3 on metapelitic assemblages at greenschist and amphibolite facies conditions: mineral equilibria calculations in the system K_2O-FeO-MgO-Al_2O_3-SiO_2-H_2O-TiO_2-Fe_2O_3. Journal of Metamorphic Geology, 18, 497-511.

Wolfram, S. (1988) Mathematica¤: A system for doing mathematics by computer. 749 p. Addison-Wesley, New, York.

Wood, B.J., Hackler, R.T., and Dobson, D.P. (1994) Experimental determination of Mn-Mg mixing properties in garnet, olivine and oxide. Contributions to Mineralogy and Petrology, 115, 438-448.

Worley, B., and Powell, R. (1998) Singularities in NCKFMASH (Na_2O-CaO-K_2O-FeO-MgO-Al_2O_3-SiO_2-H_2O). Journal of Metamorphic Geology, 16, 169-188.

Manuscript received: July 26, 2001
Manuscript published: December 17, 2001
Editorial responsibility: Frank S. Spear

Appendix 1: Mineral Formulae, Compositional Variables, and Activity-Composition Relationships

Activity models used for all MnNCKFMASH pseudosection calculations are presented below. In addition to these solid solution minerals, the pure phases quartz, zoisite, andalusite, sillimanite, kyanite, and an H_2O fluid phase were used in calculations.

Biotite: $K[Al,Fe,Mg,Mn]_1^{M1}[Fe,Mg,Mn]_2^{M2}[Si,Al]_2^{T2}Si_2O_{10}(OH)_2$

Biotite is modeled in the system MnKFMASH with the five independent end-members phlogopite (Phl), annite (Ann), eastonite (East), Mn-biotite (Mnbi), and an Fe-Mg octahedrally ordered member ordered-biotite (Obi). Biotite mixing is described by the following four variables:

$$x_1 = \left(\frac{Fe}{(Fe+Mg)}\right)^{M1}, \quad x_2 = \left(\frac{Fe}{(Fe+Mg)}\right)^{M2}, \quad y = X_{Al}^{M1}, \quad z = X_{Mn}^{M1}$$

Site fractions in terms of compositional variables are:

$$X_{Al}^{M1} = y; \quad X_{Fe}^{M1} = (1-y-z)\,x_1; \quad X_{Mg}^{M1} = (1-y-z)\,(1-x_1); \quad X_{Mn}^{M1} = z;$$

$$X_{Fe}^{M2} = (1-z)\,x_2; \quad X_{Mg}^{M2} = (1-z)\,(1-x_2); \quad X_{Mn}^{M2} = z; \quad X_{Al}^{T1} = \frac{1+y}{2}; \quad X_{Si}^{T1} = \frac{1-y}{2};$$

The ideal activities of end-members are expressed as:

$$a_{Phl}^{ideal} = 4\,X_{Mg}^{M1}\,(X_{Mg}^{M2})^2\,X_{Al}^{T1}\,X_{Si}^{T1}$$
$$a_{Ann}^{ideal} = 4\,X_{Fe}^{M1}\,(X_{Fe}^{M2})^2\,X_{Al}^{T1}\,X_{Si}^{T1}$$
$$a_{East}^{ideal} = X_{Al}^{M1}\,(X_{Mg}^{M2})^2\,(X_{Al}^{M2})^2$$
$$a_{Obi}^{ideal} = 4\,X_{Fe}^{M1}\,(X_{Mg}^{M2})^2\,X_{Al}^{T1}\,X_{Si}^{T1}$$
$$a_{Mnbi}^{ideal} = 4\,X_{Mn}^{M1}\,(X_{Mn}^{M2})^2\,X_{Al}^{T1}\,X_{Si}^{T1}$$

The proportions of each end-member in the biotite phase are defined as:

$$P_{Phl} = (1 - x_1)\,(1 - y - z)$$
$$P_{Ann} = (x_2)\,(1 - z)$$
$$P_{East} = y$$
$$P_{Obi} = 1 - y - z - (1 - x_1)\,(1 - y - z) - (1 - z)\,x_2$$
$$P_{Mnbi} = z$$

Non-ideality is expressed using symmetric formalism (Powell and Holland, 1993) with interaction parameters from Powell and Holland (1999) for KFMASH biotites. All Mnbi parameters are set to zero. The interaction parameters are (kJ/mol end-member):

$$W_{Phl-Ann} = 9;\;\; W_{Phl-East} = 10\;\; W_{Phl-Obi} = 3;\;\; W_{Ann-East} = -1;\;\; W_{Ann-Obi} = 6;\;\; W_{East-Obi} = 10;$$

Chlorite: $[Fe,Mg,Mn]_4^{M2,3}[Al,Fe,Mg,Mn]_1^{M1}[Al,Fe,Mg,Mn]_1^{M4}[Si,Al]_2^{T2}\,Si_2O_{10}(OH)_4$

Chlorite is modeled in MnFMASH with the 5 independent members Al-free chlorite (Afchl), clinochlore (Clin), amesite (Ames), daphnite (Daph), and Mn-chlorite (Mnchl). The mixing model of Holland, et al. (1998) is extended to Mn-bearing chlorites by adding the Mn-chlorite (mnchl) member, allowing Mn to mix on all octahedral sites. Compositional variables describing chlorite mixing are:

$$x_1 = \left(\frac{Fe}{Fe + Mg + Mn}\right);\;\; x_2 = \left(\frac{Mg}{Fe + Mg + Mn}\right);\;\; y = X_{Al}^{T2};\;\; N = \frac{Q}{2} = \left(\frac{X_{Al}^{M4} - X_{Al}^{M1}}{2}\right)$$

where Q is the Al ordering parameter.

Site fractions in terms of compositional variables are:

$$X_{Fe}^{M2,3} = x_1;\;\; X_{Mg}^{M2,3} = x_2;\;\; X_{Mn}^{M2,3} = (1 - x_1 - x_2);\;\; X_{Al}^{M4} = y + N;\;\; X_{Fe}^{M4} = (1 - y - N)\,x_1;$$
$$X_{Mg}^{M4} = (1 - y - N)\,x_2;\;\; X_{Mn}^{M4} = (1 - y - N)\,(1 - x_1 - x_2);\;\; X_{Al}^{M1} = y - N;\;\; X_{Fe}^{M1} = (1 - y + N)\,x_1;$$
$$X_{Mg}^{M1} = (1 - y + N)\,x_2;\;\; X_{Mn}^{M1} = (1 - y + N)\,(1 - x_1 - x_2);\;\; X_{Al}^{T2} = y;\;\; X_{Si}^{T2} = 1 - y;$$

Ideal activities of end members are expressed with mixing-on-sites, and in terms of compositional variables are expressed as:

$$a_{Afchl}^{ideal} = (x_2)^6\,(1 - y + N)\,(1 - y - N)\,(1 - y)^2$$
$$a_{Clin}^{ideal} = 4\,(x_2)^5\,(1 - y + N)\,(y + N)\,(1 - y)\,y$$
$$a_{Ames}^{ideal} = (x_2)^4\,(y - N)\,(y + N)\,(y)^2$$
$$a_{Daph}^{ideal} = 4\,(x_1)^5\,(1 - y + N)\,(y + N)\,(1 - y)\,y$$
$$a_{Mnchl}^{ideal} = 4\,(1 - x_1 - x_2)^5\,(1 - y + N)\,(y + N)\,(1 - y)\,y$$

The proportions of end-members are defined as:

$$P_{Afchl} = 1 - y - N$$
$$P_{Clin} = 2N - \tfrac{2}{5}(x_2 - 1)(y - 3)$$
$$P_{Ames} = y - N$$
$$P_{Daph} = \tfrac{2}{5} x_1 (3 - y)$$
$$P_{Mnchl} = \tfrac{2}{5}(x_1 + x_2 - 1)(y - 3)$$

Non-ideality is expressed using symmetric formalism (Powell and Holland, 1993) with updated (Holland, http://www.esc.cam.ac.uk/astaff/holland/thermocalc.html) interaction parameters from Holland, et al. (1998) for KFMASH chlorites. All Mnchl parameters are set to zero. The interaction parameters are (kJ/mol end-member):

$$W_{afchl-ames} = 20; \quad W_{clin-ames} = 18; \quad W_{clin-daph} = 3;$$
$$W_{afchl-daph} = -14.5; \quad W_{ames-daph} = 13.5; \quad W_{afchl-clin} = 18;$$

Garnet: $[Fe, Mg, Ca, Mn]_3 Al_2Si_3O_{12}$

Garnet is modeled with a quaternary regular solution between almandine (Alm), pyrope (Prp), grossular (Grs), and spessartine (Sps). The ideal activities are expressed as:

$$a_{Alm}^{ideal} = X_{Fe}^3; \quad a_{Prp}^{ideal} = X_{Mg}^3; \quad a_{Grs}^{ideal} = X_{Ca}^3; \quad a_{Sps}^{ideal} = X_{Mn}^3;$$

Non-ideality is considered between almandine and pyrope (Holland and Powell, 1998), grossular and pyrope (Vance and Holland, 1993), and spessartine and pyrope (Wood et al., 1994). The regular solution parameters are (kJ/mol):

$$W_{Alm-Prp} = 2.5; \quad W_{Grs-Prp} = 33; \quad W_{Sps-Prp} = 4.5$$

Plagioclase: $Na_x Ca_{(1-x)} Al_{(2-x)} Si_{(2+x)} O_8$ (x = 0 ↔ 1)

Plagioclase is modeled with the binary albite-anorthite solution model 4 of Holland and Powell (1992). Model 4 assumes a molecular mixing model in the $I\bar{1}$ field (high An), and a 4T-disordered model in the $C\bar{1}$ field (low An). In the $I\bar{1}$ field, ideal activities are expressed as:

$$a_{An}^{ideal} = X_{Ca}^A; \quad a_{Ab}^{ideal} = 1 - X_{Ca}^A$$

and in the $C\bar{1}$ field,

$$a_{An}^{ideal} = 16 X_{Ca}^A (X_{Al}^T)^2 (X_{Si}^T)^2; \quad a_{Ab}^{ideal} = \tfrac{256}{27} X_{Na}^A (X_{Al}^T)(X_{Si}^T)^3$$

Regular solution model interaction parameters, from Holland and Powell (1992) are (kJ/mol):

$$W_{Ab-An}^{C\bar{1}} = 5.51; \quad W_{Ab-An}^{I\bar{1}} = 9.77$$

DQF parameters, linearized in the interval 500 °C to 700 °C, are (kJ, K):

I_{an} = 4.25-0.0021*T
I_{ab} = 1.58-0.0038*T

Staurolite: $[Fe,Mg,Mn]_4\,Al_{18}Si_{7.5}O_{48}H_4$

Staurolite is modeled in MnFMAS with the 3 independent members Fe-staurolite (Fst), Mg-Staurolite (Mst), and Mn-Staurolite (Mnst), with mixing between the end-members considered ideal. Activities are expressed as:

$$a_{Mst} = X_{Mg}^4; \quad a_{Fst} = X_{Fe}^4; \quad a_{Mnst} = X_{Mn}^4$$

Chloritoid: $[Fe,Mg,Mn]Al_2SiO_5(OH)_2$

Chloritoid is modeled in MnFMAS with the 3 independent members Mg-chloritoid (Mctd), Fe-chloritoid (Fctd), and Mn-Chloritoid (Mnctd), with mixing between the end-members considered ideal. Activities are expressed as:

$$a_{Mctd} = X_{Mg}; \quad a_{Fctd} = X_{Fe}; \quad a_{Mnctd} = X_{Mn}$$

Muscovite: $[Na,K]_1^A\,[Al,Fe,Mg]_1^{M2A}\,Al\,[Al,Si]_2^{T1}\,Si_2O_{10}(OH)_2$

Muscovite is modeled in NKFMASH with the model of Holland and Powell (1998; http://www.esc.cam.ac.uk/astaff/holland/thermocalc.html). Limited substitution of Na is introduced through the fictive end-member paragonite using Darkens Quadratic Formalism. Compositional variables describing mixing are:

$$z = X_{Na}^A; \quad y = X_{Al}^{M2A}; \quad x = \left(\frac{Fe}{(Fe+Mg)}\right)^{Bulk}$$

Site fractions in terms of compositional variables are:

$$X_{Na}^A = z; \;\; X_K^A = 1-z; \;\; X_{Al}^{M2A} = y; \;\; X_{Fe}^{M2A} = (1-y)\,x;$$
$$X_{Mg}^{M2A} = (1-y)\,(1-x); \;\; X_{Al}^{T1} = \frac{y}{2}; \;\; X_{Si}^{T1} = \frac{2-y}{2};$$

Ideal activities are expressed as:

$$a_{Ms}^{Ms} = y^2\,(1-z)(2-y); \quad a_{Cel}^{ideal} = \tfrac{1}{4}(1-x)(1-y)(2-y)^2\,(1-z);$$
$$a_{Fcel}^{ideal} = \tfrac{1}{4}\,x\,(1-y)(2-y)^2\,(1-z); \quad a_{Pg}^{ideal} = y^2\,(2-y)\,z;$$

The proportions of each end-member defined in terms of compositional variables are:

$$P_{Ms} = y - z; \quad P_{Cel} = (1-x)\,(1-y);$$
$$P_{Fcel} = x\,(1-y); \quad P_{Pg} = z$$

Non-ideality is expressed with symmetric formalism. Non-ideal and DQF parameters are taken from Holland and Powell (1998; http://www.esc.cam.ac.uk/astaff/holland/thermocalc.html).

$$W_{Ms-Pg} = 12 + 0.4\,P; \;\; W_{Pg-Cel} = 14 + 0.2\,P; \;\; W_{Pg-Fcel} = 14 + 0.2\,P;$$
$$I_{Pg} = 1.42 + 0.4\,P$$

Paragonite: $NaAl_3Si_3O_{10}(OH)_2 - CaAl_4Si_2O_{10}(OH)_2$

Paragonite is modeled in NCASH using expressions supplied with program THERMOCALC (v.2.7). The model utilizes Darkens Quadratic Formalism to allow a limited amount of Ca substitution through the fictive end-member margarite. Mixing between paragonite and margarite is limited to the Na-Ca exchange vector; Al and Si mixing is not considered. Paragonite and margarite are considered to mix ideally except for the DQF increment applied to margarite. Activity expressions and the DQF increment are:

$$a_{Pg} = X_{Na}; \quad a_{Mrg} = X_{Ca}; \quad I_{Mrg} = 12.0$$

Cordierite: $[Fe,Mg,Mn]_2\, Al_4Si_5O_{18} \cdot H_2O$

Cordierite is modeled in MnFMASH with the four end-members Mg-cordierite (Crd), Fe-cordierite (Fcrd), Mn-cordierite (Mncrd), and hydrous Mg-cordierite (Hcrd). All end-members are considered to mix ideally. Compositional variables are defined as:

$$x = \left(\frac{Fe}{(Fe + Mg + Mn)}\right)^{Bulk}; \quad mn = \left(\frac{Mn}{(Fe + Mg + Mn)}\right)^{Bulk}; \quad h = X_{H_2O}$$

Activities are expressed as:

$$a_{Crd} = (1 - x - mn)^2\,(1 - h); \quad a_{Fcrd} = x^2\,(1 - h);$$
$$a_{Mncrd} = mn^2\,(1 - h); \quad a_{Hcrd} = (1 - x - mn)^2\,h$$

Alkali Feldspar: $[Na,K]AlSi_3O_8$

Alkali feldspar is modeled with a binary sub-regular solution model between the end-members sanidine (Sa) and albite (Ab) using expressions supplied with program THERMOCALC (v.2.7). Ideal activities are expressed as:

$$a_{Sa}^{ideal} = X_K^A; \quad a_{Ab}^{ideal} = X_{Na}^A$$

Non-ideal mixing parameters are:

$$W_{Sa-Ab} = 26.5 - 0.01825 \cdot T + 0.3870 \cdot P;$$
$$W_{Ab-Sa} = 32.1 - 0.01614 \cdot T + 00469 \cdot P$$

Appendix 2. Thermobarometry Methods

Pressures and temperatures of metamorphism for 18 Waterville Fm. samples were calculated using mineral compositions reported in Ferry (1980). Pressures and temperatures were constrained by the GASP barometer and GaBi thermometer, respectively.

$$\text{Grs} + 2\ \text{And/Sil} + \text{Qtz} = 3\ \text{An} \qquad \text{GASP}$$

$$\text{Prp} + \text{Ann} = \text{Alm} + \text{Phl} \qquad \text{GaBi}$$

Iterative routines coded in Mathematica (Wolfram, 1988) were used to solve the following equilibrium relationships for pressure and temperature, respectively:

$$0 = \Delta G^{0}_{GASP} + R\,T\,Ln\frac{a^{3}_{An}}{a_{Grs}} \qquad \text{GASP}$$

$$0 = \Delta G^{0} + R\,T\,Ln\frac{a_{Alm}\,a_{Phl}}{a_{Prp}\,a_{Ann}} \qquad \text{GaBi}$$

To solve the GASP expression above for pressure, ΔG^{0}_{GASP} was linearised in the form $a + b\,T + c\,P$ at the equilibrium pressure and temperature of the previous iteration.

Garnet and plagioclase activity models are the same as those used in the pseudosections. The pseudosection biotite activity model was modified to allow mixing of Ti on the same octahedral site as Al before the Fe-Mg ordering calculations were performed. All Ti interaction parameters were set to zero. Activities and equilibrium relationships were calculated to within 1 °C and 10 bars of the final P-T solution.